Accepted Manuscript

Synthesis, structure-activity relationship studies and biological characterization of new [1,2,4]triazolo[1,5-*a*]pyrimidine-based LSD1/KDM1A inhibitors

Shuai Wang, Zhong-Rui Li, Feng-Zhi Suo, Xiao-Han Yuan, Bin Yu, Hong-Min Liu

PII: S0223-5234(19)30153-9

DOI: https://doi.org/10.1016/j.ejmech.2019.02.039

Reference: EJMECH 11131

To appear in: *European Journal of Medicinal Chemistry*

Received Date: 5 November 2018

Revised Date: 13 January 2019

Accepted Date: 10 February 2019

Please cite this article as: S. Wang, Z.-R. Li, F.-Z. Suo, X.-H. Yuan, B. Yu, H.-M. Liu, Synthesis, structure-activity relationship studies and biological characterization of new [1,2,4]triazolo[1,5-*a*]pyrimidine-based LSD1/KDM1A inhibitors, *European Journal of Medicinal Chemistry* (2019), doi: https://doi.org/10.1016/j.ejmech.2019.02.039.

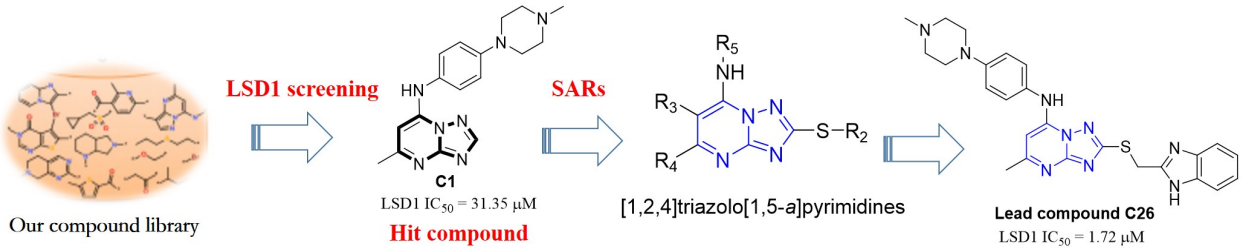

Our compound library

Synthesis, structure-activity relationship studies and biological characterization of new [1,2,4]triazolo[1,5-*a*]pyrimidine-based LSD1/KDM1A inhibitors

Shuai Wang [a,c,d,#], *Zhong-Rui Li* [a,c,d,#], *Feng-Zhi Suo* [a,c,d], *Xiao-Han Yuan* [a,c,d], *Bin Yu* [a,b,c,d,*], *and Hong-Min Liu* [a,c,d,*].

[a] *School of Pharmaceutical Sciences, Zhengzhou University, Zhengzhou 450001, China;*

[b] *State key Laboratory of Pharmaceutical Biotechnology, Nanjing University, Nanjing 210023, Jiangsu, People's Republic of China.*

[c] *Key Laboratory of Advanced Drug Preparation Technologies (Ministry of Education), Zhengzhou University, Zhengzhou 450001, China;*

[d] *Co-Innovation Center of Henan Province for New Drug R & D and Preclinical Safety, Zhengzhou University, Zhengzhou 450001, China;*

* **Corresponding authors**:

Dr. Bin Yu (zzuyubin@hotmail.com)

Prof. Hong-Min Liu (liuhm@zzu.edu.cn)

[#] *Shuai Wang and Zhong-Rui Li contributed equally to this work.*

Abstract: The histone lysine specific demethylase 1 (LSD1/KDM1A) is implicated in the development of cancers, targeting LSD1 has been recognized as a promising strategy for cancer therapy. To date, some small-molecule inhibitors are currently being investigated in clinical trials. Herein we report the design, synthesis and biochemical characterization of [1,2,4]triazolo[1,5-*a*]pyrimidine derivatives as new LSD1 inhibitors. Of these compounds, compound **C26** inhibited LSD1 in a reversible manner (IC_{50} = 1.72 μM) and showed selectivity to LSD1 over MAO-A/B. Besides, compound **C26** displayed FAD-competitive binding to LSD1. Interestingly, **C26** did not inhibit horseradish peroxidase (HRP) and quench H_2O_2, thus excluding the possibility that LSD1 inhibition by **C26** was due to the HRP inhibition and consumption of H_2O_2. In LSD1 overexpressed A549 cells, compound **C26** concentration-dependently induced accumulation of H3K4me1/me2 and H3K9me2 and showed cellular target engagement to LSD1. Additionally, compound **C26** significantly inhibited migration of A549 cells in a concentration-dependent manner, further western blot analysis showed that **C26** increased expression levels of epithelial cell markers E-Cadherin and Claudin-1, down-regulated mesenchymal cell marker N-Cadherin and the upstream transcription factors Snail and Slug. Docking studies were also performed to rationalize the potency of **C26** toward LSD1. To conclude, the [1,2,4]triazolo[1,5-*a*]pyrimidine could serve as a promising scaffold for the development of new LSD1 inhibitors.

Keywords: [1,2,4]triazolo[1,5-*a*]pyrimidines; LSD1 inhibitors; Antiproliferative activity; Migration inhibition;

1. Introduction

Histone lysine specific demethylase LSD1 (also known as KDM1A) was first identified in 2004 by Professor Shi Yang [1]. As a monoamine oxidase homologue, LSD1 specifically removes methyl groups of H3K4/H3K9, thereby causing activation or suppression of genes [2]. LSD1 is highly expressed in many tumor cells [3, 4]. Abnormally high expression of LSD1 promotes tumorigenesis by regulating chromatin (such as chromatin remodeling and aggregation) [5]. In addition, high expression of LSD1 can lead to inhibition of p53 function by inhibiting the interaction between p53 and TP53BP1 (p53 binding protein 1) [6], which then affects the cancer cell cycle [7], promotes tumor growth, invasion and metastasis by affecting the methylation/demethylation process [8-10]. Therefore, targeting LSD1 is becoming an important therapeutic strategy for cancer therapy [11]. To date, a large number of natural and synthetic LSD1 inhibitors [12-23] have been identified, of which 2-PCPA, phenelzine, and pargyline [24-27] were initially found to be able to inhibit LSD1 irreversibly. Subsequent modifications based on the 2-PCPA scaffold have generated numerous covalent LSD1 inhibitors. Encouragingly, GSK-2879552 [28, 29], ORY-1001 [30], IMG-7289, CC-90011, INCB059872 [31, 32] and ORY-2001 have advanced into clinical trials. Based on our previous work on the identification of LSD1 inhibitors [33-41], herein we report the design, synthesis and biological characterization of [1,2,4]triazolo[1,5-*a*]pyrimidine derivatives as new LSD1 inhibitors, of which compound **C26** inhibited LSD1 in a reversible manner and was also on target in A549 cells.

2. Results and Discussion

2.1. Chemistry

The synthetic routes for the synthesis of compounds C1-C32. As shown in Scheme 1, 4*H*-1,2,4-triazol-3-amine reacted with different *β*-ketoesters in acetic acid generated compounds **A1**-**A4**, which were then subjected to the chlorination reaction in $POCl_3$, affording compounds **B1**-**B4**. Subsequent substitution reactions of **B1**-**B4** with 4-(4-methylpiperazino)aniline yielded compounds **C1**-**C4**. Starting from 5-amino-4*H*-1,2,4-triazole-3-thiol, the intermediates **D1**-**D22** were obtained through

the substitution reactions with various alkyl halides. Compounds **D1**-**D22** then reacted with diverse β-ketoesters to generate compounds **A5-A29**. Chlorination of compounds **A5**-**A29** in $POCl_3$ formed compounds **B5-B29**, which then reacted with commercially available amines to form the corresponding compounds **C5-C32.**

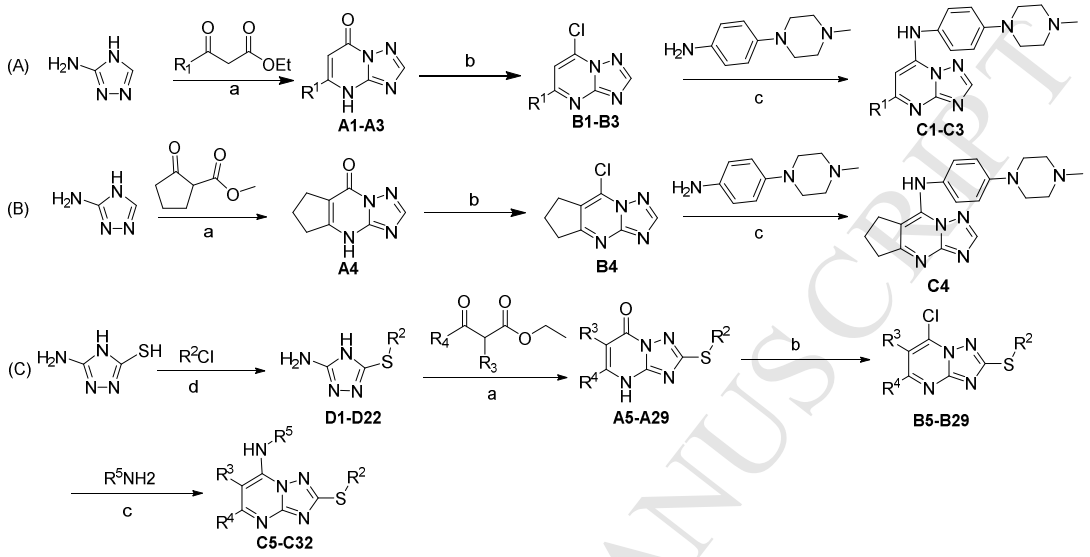

Scheme 1. Synthesis of compounds **C1-C32**. Reagents and conditions: (a) Acetic acid, 120 ^{o}C, 2-15 h, reflux. (b) $POCl_3$, 90 ^{o}C, 3-5 h, reflux; (c) Et_3N, EtOH, rt, 5 h; (d) Na_2CO_3, acetone, 60 ^{o}C, 3-5 h, reflux.

2.2. SARs investigations

Based on our previously established screening methods against LSD1 [40], we screened our in-house library using GSK2879552 as a control compound (LSD1 IC_{50} = 24 nM) [42], leading to the discovery of hit compound **C1,** which inhibited LSD1 with an IC_{50} value of 31.35 μM (Fig. 1). Initial modifications focused on the replacement of the methyl group with more steric ethyl and phenyl groups, generating compounds **C2** and **C3** with decreased anti-LSD1 activity (IC_{50} = 38.13 and >50 μM, respectively). Besides, the cyclopentane fused compound **C4** was also inactive against LSD1 (IC_{50} > 50 μM). The results suggest that the less steric group (e.g. –Me) was preferred for the activity.

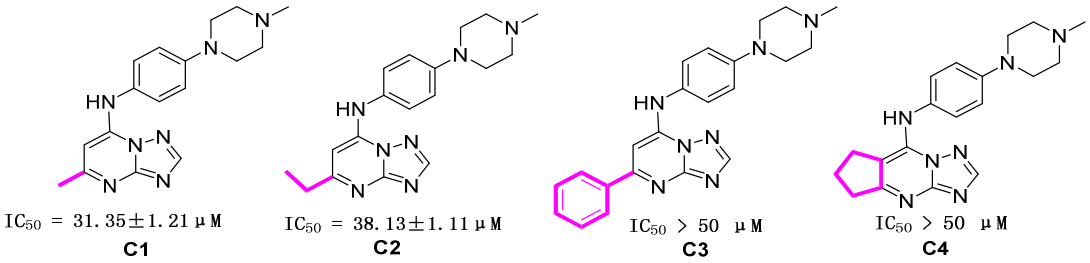

Fig. 1. Initial modifications based on the [1,2,4]triazolo[1,5-*a*]pyrimidine scaffold.

With compound **C1** in hand, we then performed further SARs studies as shown in Fig. 2. Aniline and $–NH_2$ substituted compounds **C30** and **C31** exhibited decreased activity (IC_{50} > 50 μM) compared to the hit compound **C1**, indicating the importance of the hydrophilic *N*-methylpiperazine group for the activity. This finding is consistent with previous reports [12, 27, 43-47], namely, the hydrophilic groups such as piperidine, piperazine, *etc*. always exist in some highly potent and selective LSD1 inhibitors (e.g. ORY-1001, GSK-2879552, etc.). Intriguingly, the introduction of the benzyl mercapto group to the [1,2,4]triazolo[1,5-*a*]pyrimidine scaffold led to the increase of the anti-LSD1 activity by a fact of about 2.5. Compound **C5** inhibited LSD1 with an IC_{50} value of 12.39 μM. Compounds **C19** and **C20** bearing the $–(CH_2)_2Ph$ and $–(CH_2)_3Ph$ moiety, respectively displayed significantly decreased anti-LSD1 activity compared to **C1**, underscoring the importance of the length of the side chain for the activity. To our surprise, compounds **C28** and **C29** possessing additional methyl and *n*-pentyl groups were found to be inactive against LSD1 (IC_{50} > 50 μM).

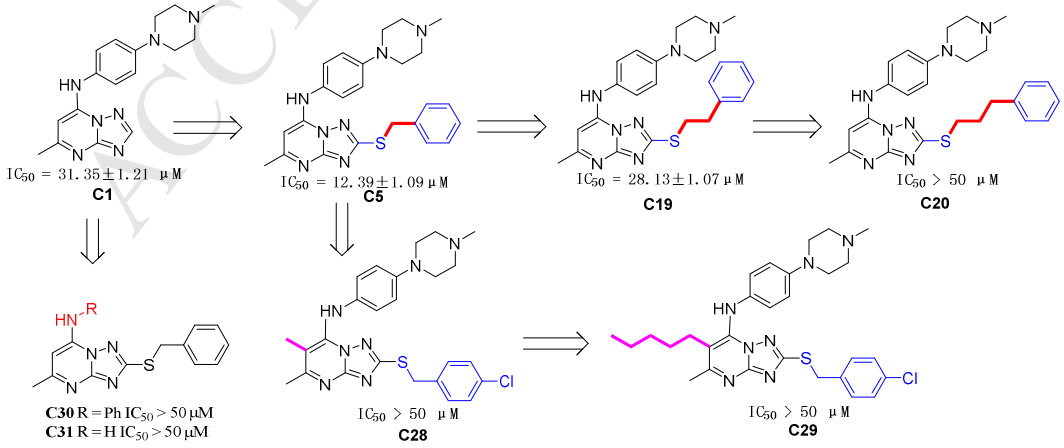

Figure 2. Further optimization based on the hit compound **C1**.

Molecular fine-turning on the phenyl ring of **C5** was further carried out, generating compounds **C6**-**C18** and **C26**-**C27**. As shown in Fig. 3, the incorporation of halo atom into the phenyl ring caused decrease of the anti-LSD1 activity. Compounds **C6**-**C10**, **C14**-**C16**, and **C18** showed moderate inhibition against LSD1 with the IC_{50} values ranging from 18 to 30 μM, slightly less potent than **C5**. While the $–NO_2$ containing compounds **C11** and **C12** displayed significantly decreased activity with the IC_{50} value of 32.56 and >50 μM, respectively. The –OMe and –Me containing compounds **C13** and **C17** also exhibited decreased activity with the IC_{50} values of 17.38 and 25.78 μM, respectively. Compound **C18** bearing the $–CF_3$ group showed comparable inhibitory activity with **C5**. Interestingly, replacement of the phenyl ring in **C5** with benzimidazole and benzothiophene formed **C26** and **C27** (Fig. 4), of which **C26** inhibited LSD1 with an IC_{50} value of 1.72 μM. To our surprise, removal of *N*-methylpiperazine group in compound **C26** generated compound **C32**, which showed with significantly decreased anti-LSD1 activity (IC_{50} > 50 μM), the data unveiled the importance of the hydrophilic *N*-methylpiperazine group for the activity. We also found that replacement of the benzyl ring with other aliphatic groups caused decrease of the activity (Fig. 4). Compound **C23** bearing a terminal alkyne group showed comparable activity (IC_{50} = 14.84 μM) with **C5**.

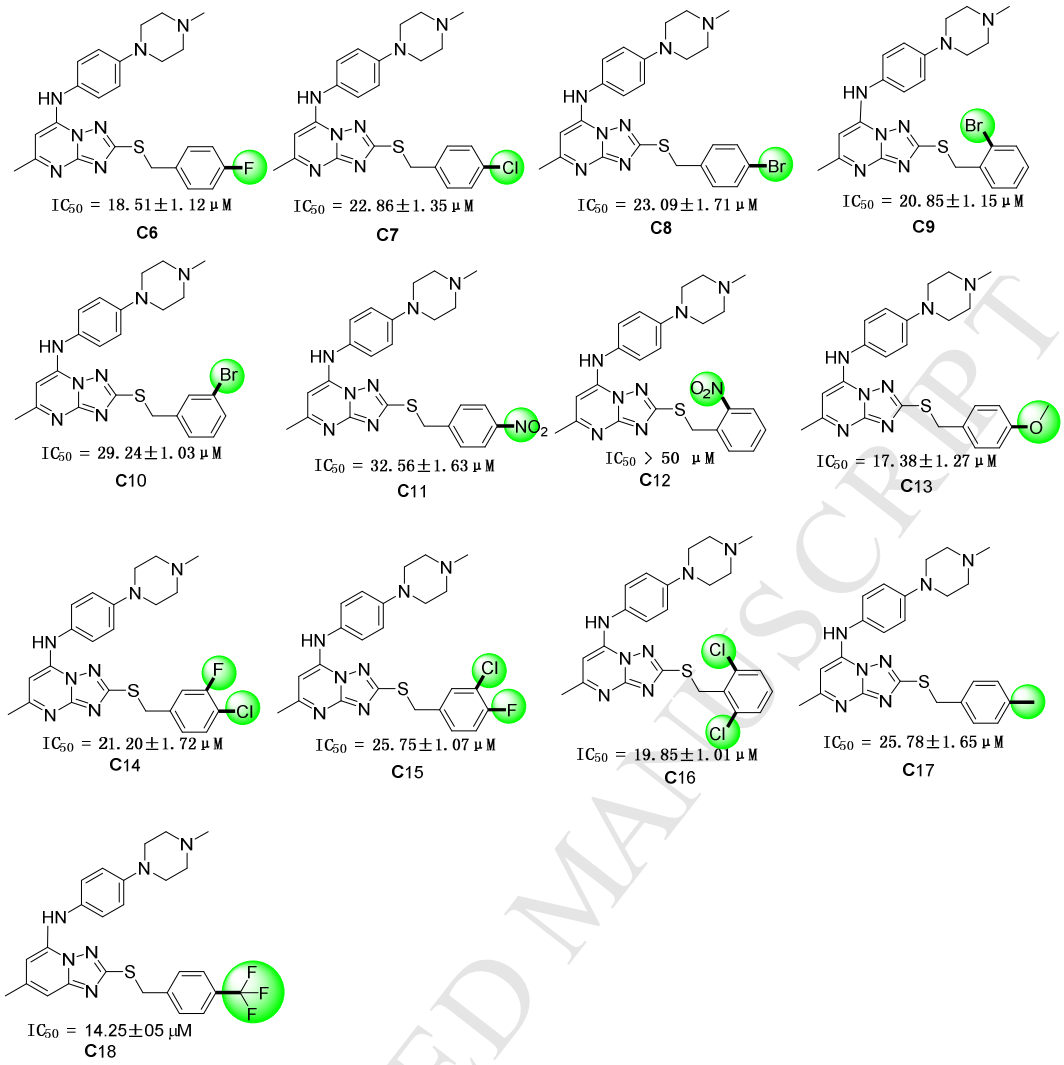

Figure 3. Structural modifications on the phenyl ring of **C5**.

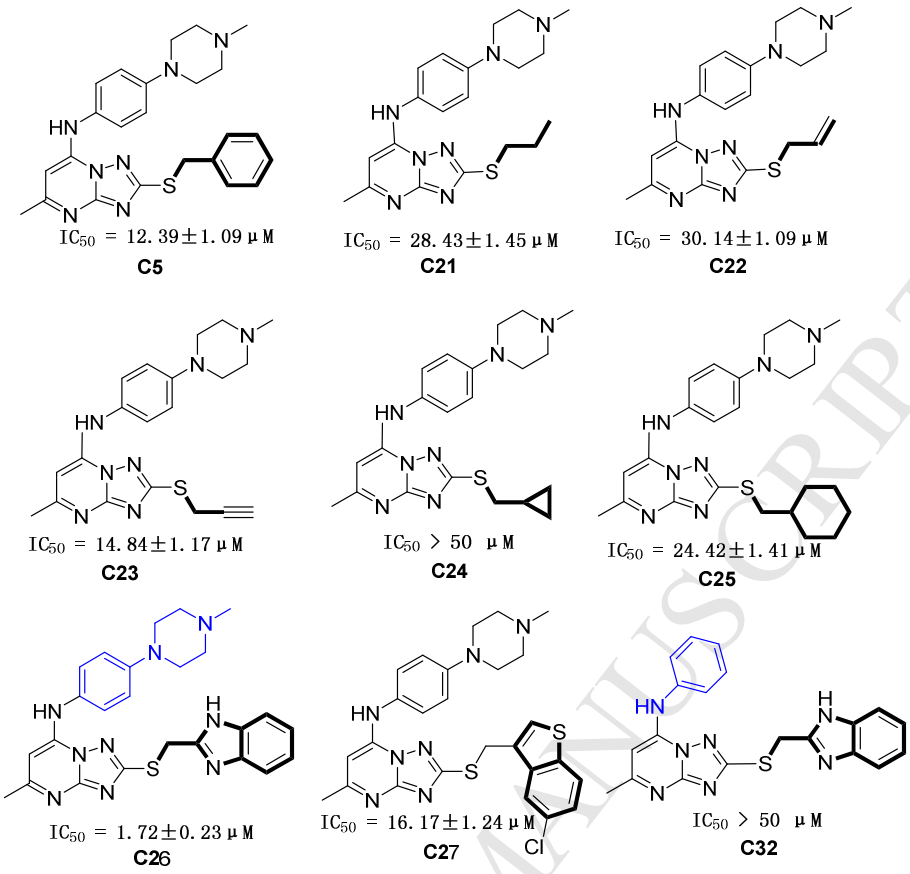

Figure 4. Structures and biochemical potency of compounds **C5** and **C21-C27**.

*2.3. Biochemical characterization of **C26***

The assay procedure used in this work couples the production of H_2O_2 from the LSD1 reaction with horseradish peroxidase (HRP), the product of which is then captured by Amplex Red. While the drawback of this commonly used assay procedure is that compounds with aromatic character often act as HRP inhibitors, giving a false positive reading [48]. This interaction can make it appear that a compound inhibits LSD1, when in fact it only inhibits HRP. We first detected the inhibitory effect of **C26** on HRP, as shown in Fig. 5A, **C26** did not inhibit HRP even at 10 μM, thus excluding false positive results caused by HRP inhibition. Additionally, compounds that quench H_20_2 could also falsely show LSD1 inhibition [49]. We next examined whether the thioether **C26** could quench H_20_2 using a structurally similar but inactive compound **C32** (IC_{50} > 50 μM) as a control. As shown in Fig. 5B, both compounds could not quench H_2O_2, thus excluding the possibility that LSD1 inhibition by **C26** was due to the consumption of H_2O_2. In view of the acceptable potency of **C26** against LSD1, we

first examined inhibitory effects of compound **C26** against MAO-A/B as LSD1 shares similar amino acid sequence with MAO-A/B [50, 51]. We found that compound **C26** inactivated MAO-A 40% at 10 μM and 13% at 1 μM (Fig. 5C). Meanwhile, we also observed that compound **C26** inactivated MAO-B 34% at 10 μM and 18% at 1 μM. These results indicated that compound **C26** had certain selectivity to LSD1 over MAO-A/B. Next, a dilution assay was performed to examine the reversibility of compound **C26** against LSD1 using GSK2879552 as the control compound [28], which is a potent, selective, mechanism-based LSD1 inactivator (ClinicalTrials.gov Identifier: NCT02929498). As shown in Fig. 5D, 80-fold dilution of the LSD1/compound **C26** mixture resulted in the recovery of LSD1 activity, suggesting reversible binding of **C26** to LSD1. In contrast, the covalent LSD1 inhibitor GSK2879552 failed to recover the anti-LSD1 activity after dilution. It is well recognized that LSD1 inhibitors could competitively bind to LSD1 with FAD or histone substrates (e.g. H3K4me2) [52]. Herein we performed the competitive analysis of compound **C26** within the active site of LSD1. As depicted in non-linear regression analysis (Figs. 5E and 5F), compound **C26** competitively bound to LSD1 with FAD (Fig. 5F), while it showed a noncompetitive binding with H3K4me2 (Figure Fig. 5E). These results indicated that compound **C26** may occupy the binding pocket that FAD stands, finally leading to decrease of the demethylase activity of LSD1. To conclude, compound **C26** was a reversible and FAD-competitive LSD1 inhibitor.

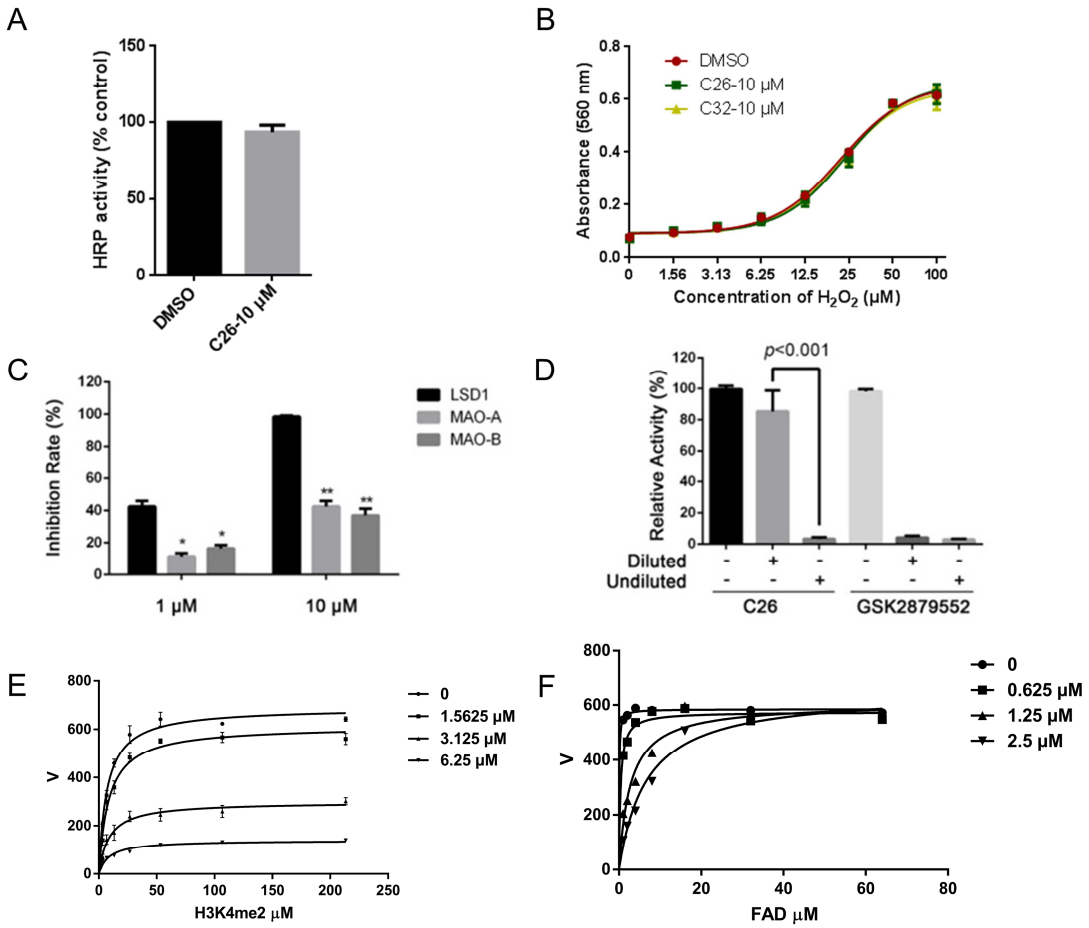

Figure 5. Biochemical characterization of compound **C26** toward LSD1 activity in vitro. (A) The effect of **C26** on HRP activity. (B) H_2O_2 quantitation curve of **C26** and **C32** was measured by ferrous ion oxidation-xylenol orange (FOX) method. (C) Selectivity of compound **C26** to LSD1 over MAO-A/B. (D) The reversibility of compound **C26** (40 μM) to LSD1 was determined by the dilution assay, GSK2879552 (1.6 μM) was used as a control. (E, F) The non-linear regression analysis demonstrated that compound **C26** is noncompetitive with the histone H3 substrate (E) and competitive with the LSD1 cofactor FAD (F). Data are mean ± SD. $P < 0.01$ was considered statistically highly significant. All experiments were carried out at least three times.

*2.4. Cellular effects of compound **C26** in LSD1 overexpressed A549 cells*

It has been reported that LSD1 is highly expressed in human lung cancer cells [28, 51, 53]. It is well known that LSD1 can catalytically remove the methyl groups of LSD1 substrates H3K4me1/2 and H3K9 me1/2 [3]. Herein we investigated the effects of

compounds **C26**, **C32** (inactive control) and **GSK-LSD1** (positive control) on the methylation of histone substrates H3K4me1/2 and H3K9 me1/2 in LSD1 overexpressed A549 cells. As demonstrated in Figs. 6A and 6C, compounds **C26** and **GSK-LSD1** concentration-dependently induced accumulation of H3K4me1/2 and H3K9 me1/2 in A549 cells after treatment for 96 h. In contrast, the inactive compound **C32** was ineffective in modulating methylation of H3 peptide substrates in A549 cells (Fig. 6B). These results proved that **C26** was cellularly active.

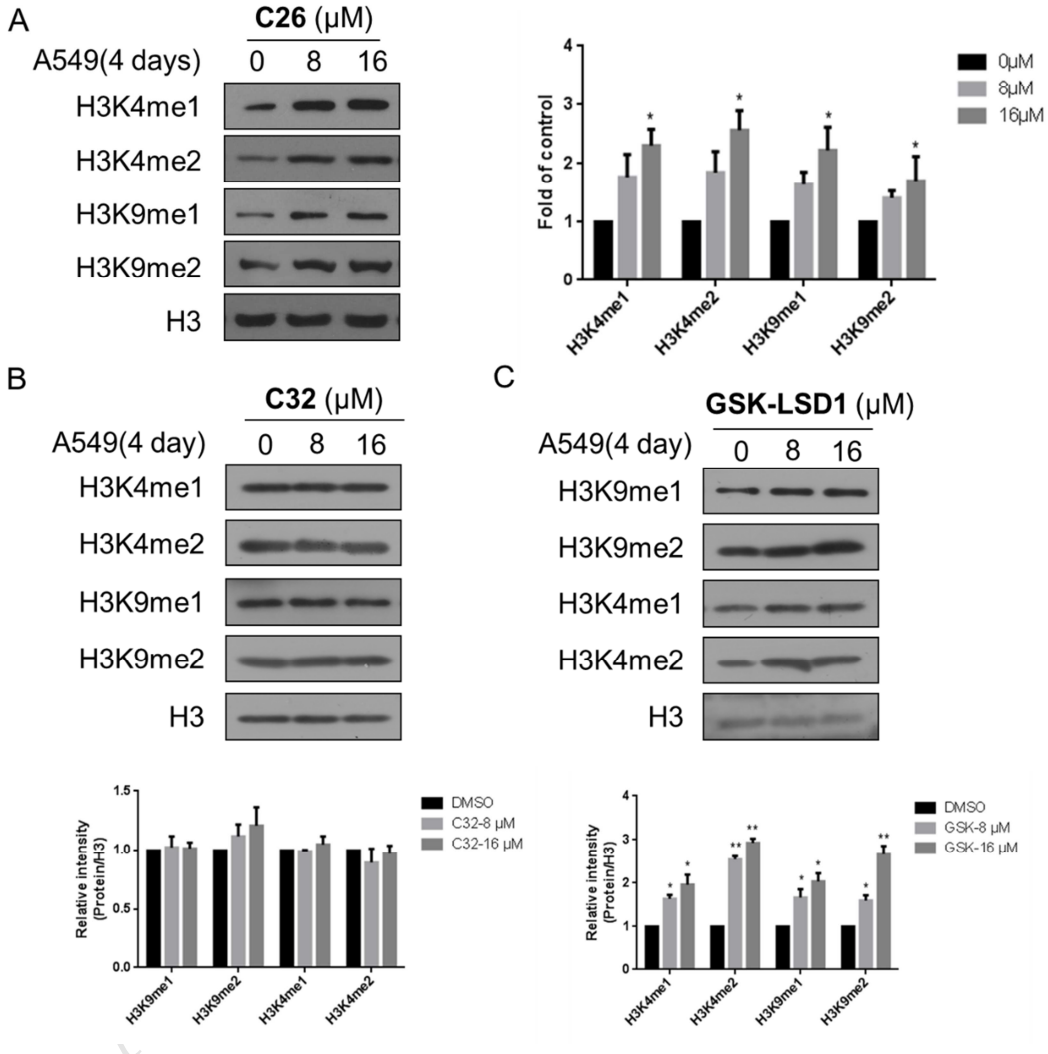

Figure 6. Histone methylation in A549 cells after treatment with **C26** (A), **C32** (B) and **GSK-LSD1** (C) for 4 days. The expressions of H3K4me1/2 and H3K9me1/2 were determined by western blot. The total levels of histone (H3) were used as loading control. (*) $P < 0.05$ was considered statistically significant. (**) $P < 0.01$ was considered statistically highly significant. All experiments were carried out at

least three times.

In order to further validate the cellular target engagement of **C26** in A549 cells, we employed the cellular thermal shift assay (CETSA) [54] to examine whether **C26** treatment could increase thermal stability of LSD1 using **GSK-LSD1** as a positive control (Fig. 7). As expected, **GSK-LSD1** increased the stability of cellular LSD1 at 49 and 52 ^{o}C at 10 μM (Fig. 7C). As shown in Fig. 7A, treatment with **C26** (10 and 20 μM) at 46 and 49 ^{o}C increased stability of cellular LSD1. Particularly, compound **C26** significantly increased cellular thermal stability of LSD1 in A549 cells at 52 ^{o}C compared to the group treated with DMSO, while the cellular LSD1 protein was denatured at 52 °C in A549 cells with DMSO treatment. In contrast, after treatment with the negative compound **C32** (10 μM), the thermal stability of cellular LSD1 was similar to that of the DMSO group (Fig. 7B). This data suggested that **C26** was on target to LSD1 in A549 cells.

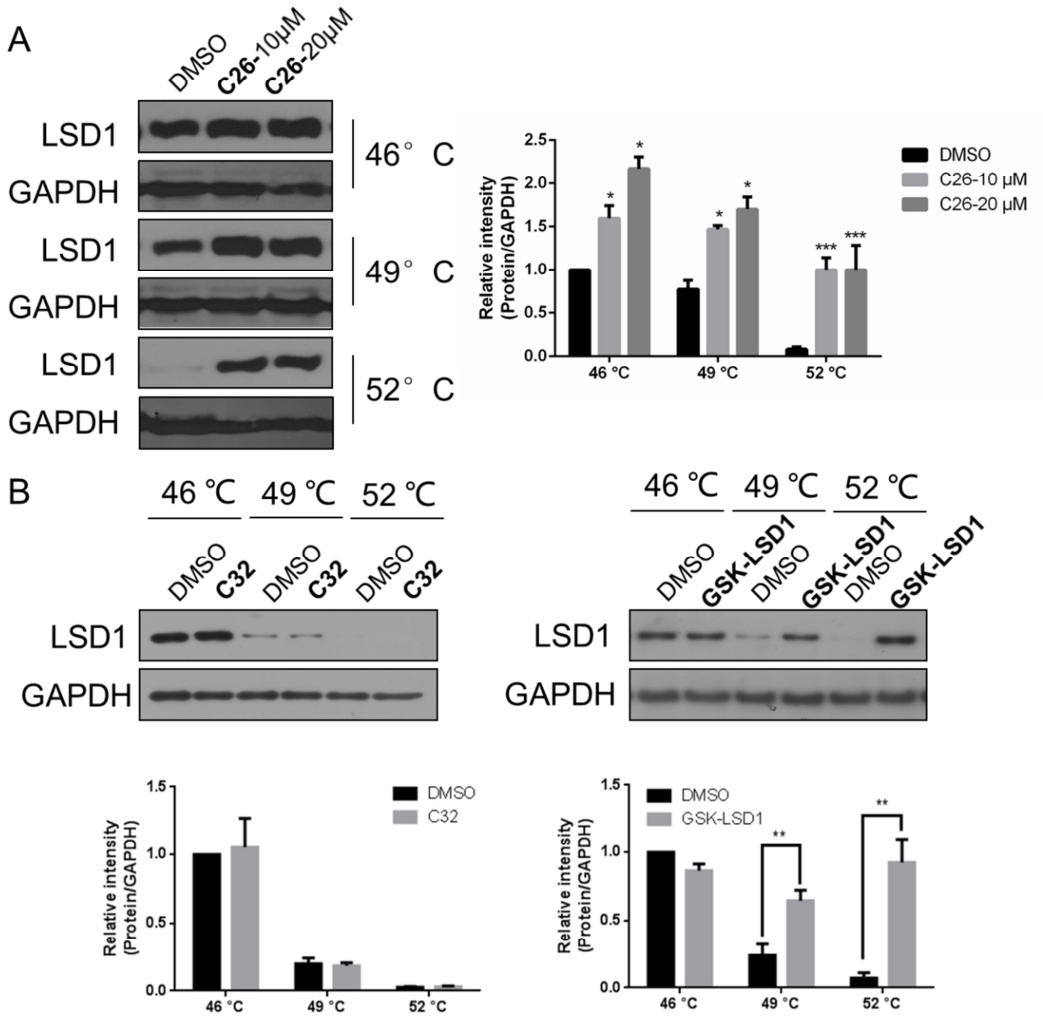

Figure 7. Cellular target engagement of **C26** in A549 cells. (A) **C26** (10, 20 μM), (B) **C32** (10 μM) and (C) **GSK-LSD1 (**10 μM) were used in cellular thermal shift assay (CETSA). A549 cells were treated with compound **C26** for 1 h, followed by heating at different temperatures for 3 min. Protein levels of LSD1 were examined by the western blotting analysis. GAPDH was used as a loading control. (*) $P < 0.05$ was considered statistically significant. (***) $P < 0.01$ was considered statistically highly significant. All experiments were carried out at least three times.

In view of the acceptable potency against LSD1 and cellular target engagement of **C26** in A549 cells, we also evaluated the effect on the cell viability of A549 cells. As shown in Fig. 8, **GSK-LSD1** had no effect on the cell viability even at high concentration, while compound **C26** concentration-dependently reduced the cell

viability of A549 cells with an IC_{50} value of 23.76 μM. The negative compound **C32** did not affect the cell viability of A549 cells at < 40 μM, **C32** at higher concentration caused significantly decreased cell viability. The decreased cell viability induced by **C26** may be partly due to the LSD1 inhibition.

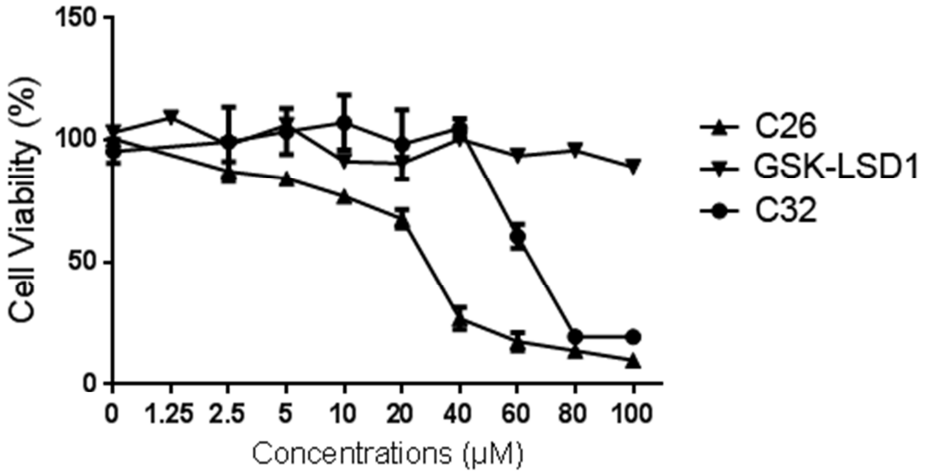

Figure 8. The effect of **C26, C32 and GSK-LSD1** on the cell viability of A549 cells.

*2.5. Migration inhibition of compound **C26** against A549 cells*

As reported previously, LSD1 was involved in epithelial-mesenchymal transition (EMT), which contributed to the migration and invasion of cancer cells [55, 56]. Therefore, the high content analysis was performed to examine the effect of **C26** on the migration of A549 cells using **GSK-LSD1** and **C32** as the controls. As shown in Fig. 9A, compound **C26** significantly inhibited migration of A549 cells in a concentration-dependent manner, especially at 16 μM. We also examined the expression of the typical proteins of EMT process (Fig. 9B), showing that compound **C26** up-regulated the epithelial cells biomarkers, E-Cadherin and claudin-1, while the mesenchymal cells biomarker N-Cadherin was down-regulated correspondingly. Then the upstream transcription factors Snail and Slug were also down-regulated after treatment with compound **C26**, indicating that compound **C26** may regulate the biomarkers of the EMT process through inhibiting the expression of the transcription factors and then cause the interference of EMT process ultimately. At the same time, typical proteins of the EMT process were also examined after treatment with **C32** and **GSK-LSD1**. As shown in Fig. 9C, **C32** had no effect on the expression of these

proteins in A549 cells. Like **C26**, **GSK-LSD1** also inhibited the EMT process**,** accompanied by up-regulation of E-Cadherin and claudin-1 as well as down-regulation of *N*-Cadherin, Snail, and Slug (Fig. 9D). As expected, the inactive compound **C32** did not affect the expression levels of the EMT-related proteins. We also found that **C26**, **C32** and **GSK-LSD1** did not affect expression of LSD1.

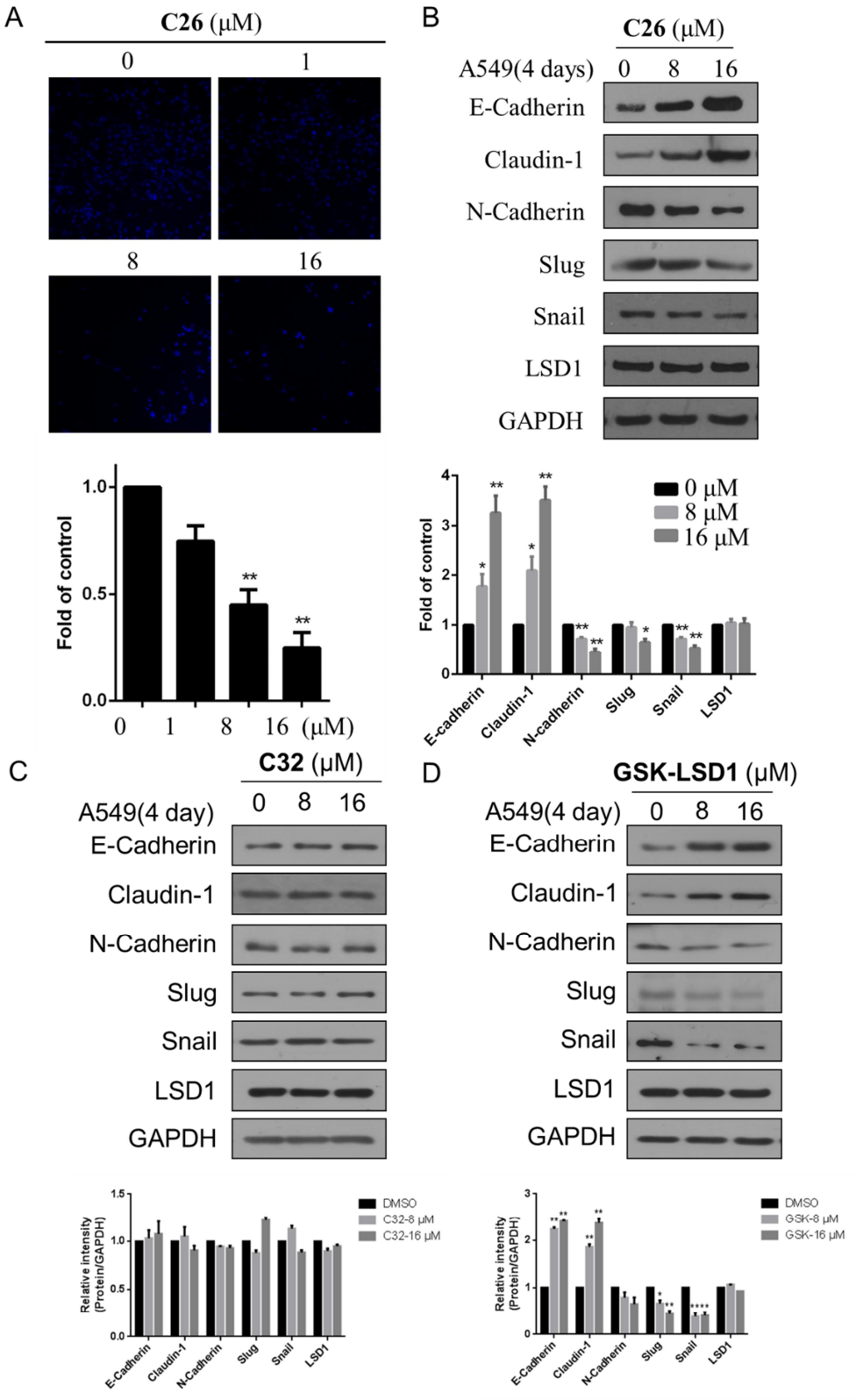

Figure 9. The effect of compounds **C26, C32** and **GSK-LSD1** on the migration of A549 cells and expression levels of key proteins. (A) Migration ability assay. Treatment of compound **C26** resulted in the migration inhibition. The expressions of E-Cadherin, Claudin-1, N-Cadherin, Slug, Snai1 and LSD1 after treatment with

compound **C26** (B)**, C32** (C) **and GSK-LSD1** (D) for 96 h. GAPDH was used as loading control. (∗) $P < 0.05$ was considered statistically significant. (∗∗) $P < 0.01$ was considered statistically highly significant. All experiments were carried out at least three times.

2.6. Molecular docking studies

In order to rationalize the potency of compound **C26** against LSD1, the crystal structure (PDB code: 2v1d) of LSD1 in complex with CoREST and a substrate-like peptide inhibitor [57] was downloaded from the RCSB database and used as a receptor for the docking studies. As shown in Fig. 10A, compound **C26** (colored in green) occupied the hydrophobic tabular cavity of LSD1, showing overlap with FAD (colored in yellow). The predicted modeling further confirmed FAD-competitive binding mode as shown in the Lineweaver−Burk plots (Figs. 5E and 5F). The binding models indicate that the 3D geometry of **C26** may play critical roles in the anti-LSD1 activity. As shown in Fig. 10B, the aromatic triazolo[1,5-*a*]pyrimidine ring laying at the central of the pocket formed two π-H interactions, one of the nitrogen atom of the pyrimidine ring also had an interaction with Val288. The NH attached to the triazolo[1,5-*a*]pyrimidine ring formed an hydrogen bond with Arg316. These interactions may be important in maintaining the preferred 3D geometry. Additionally, the benzimidazole NH and the protonated *N*-Me piperazine NH had an H-bond interaction with Glu308 and Met4, respectively. The predicted binding models may provide structural basis for further structure-based modifications.

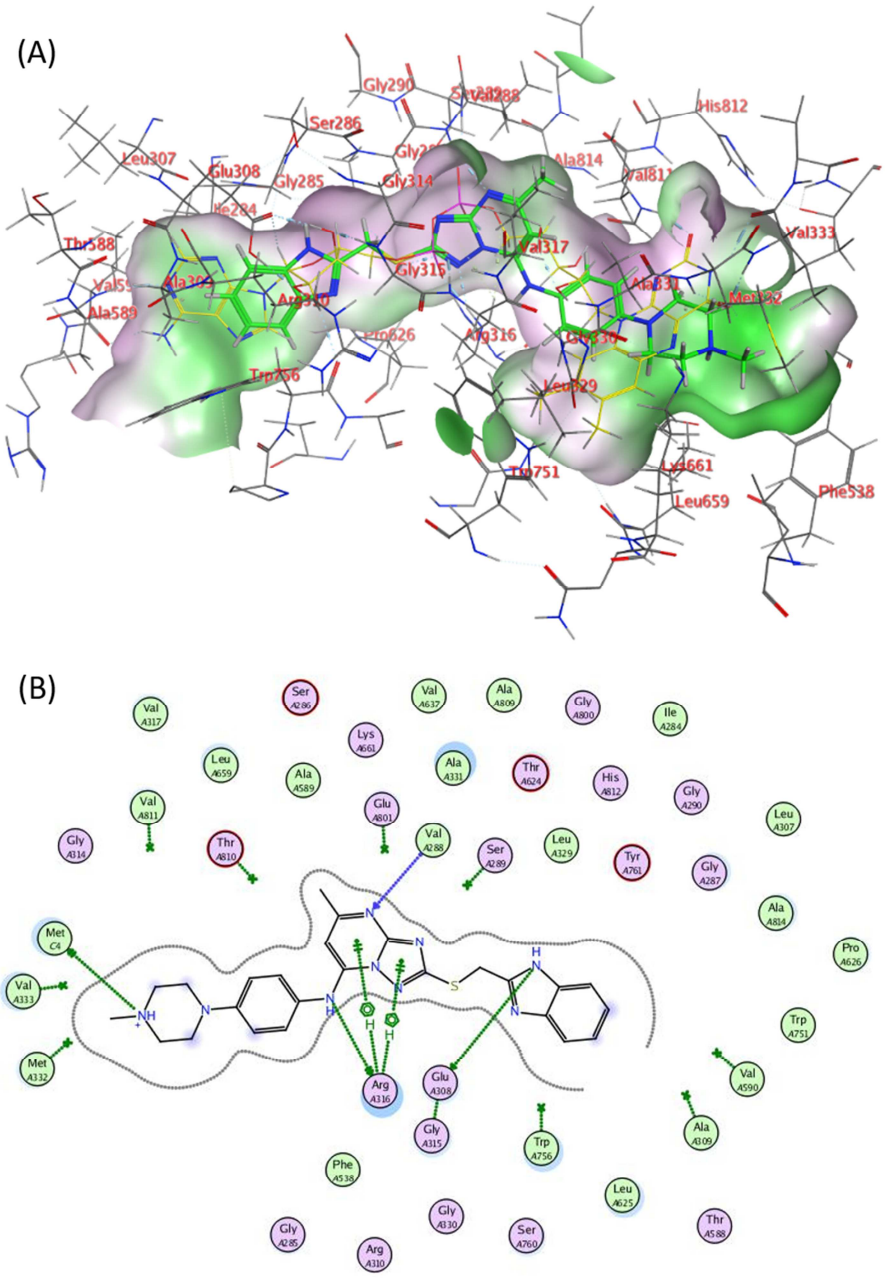

Figure 10. Molecular docking studies of **C26** in the active site of LSD1. (A) Three-dimensional binding models of **C26** in the active site of LSD1 (PDB code: 2v1d). FAD and **C26** were colored in yellow and green, respectively. The hydrophobic region of LSD1 was colored in green, while the hydrophilic region was colored in purple; (B) Two-dimensional (2D) interaction diagram of **C26** with surrounding residues, the 2D diagram was generated with the MOE software. Green dashed lines indicate hydrogen bonds, blue dashed line represents backbone acceptor.

3. Conclusions

A new series of 4-(*N*-methylpiperazin-1-yl)aniline substituted [1,2,4]triazolo[1,5-*a*]pyrimidine derivatives were synthesized and evaluated for their anti-LSD1 activity. Based on the initially identified hit compound, further medicinal chemistry efforts led to the discovery of compound **C26**, which inhibited LSD1 (IC_{50} = 1.72 μM) in a reversible manner, showed selectivity to LSD1 over MAO-A/B, but did not inhibit HRP or quench H_2O_2, excluding the false positive results. Besides, compound **C26** competitively bound to LSD1 with FAD, while it showed a noncompetitive binding with H3K4me2. In LSD1 overexpressed A549 cells, compound **C26** concentration-dependently induced accumulation of LSD1 substrates - H3K4me1/me2 and H3K9me2 and showed cellular target engagement to LSD1. Additionally, compound **C26** significantly inhibited migration of A549 cells in a concentration-dependent manner, further western blot analysis showed that **C26** increased expression levels of epithelial cell markers E-Cadherin and Claudin-1, down-regulated mesenchymal cell marker N-Cadherin and the upstream transcription factors Snail and Slug. Docking studies were also performed to rationalize the potency of **C26** toward LSD1, suggesting that **C26** occupied FAD binding site of LSD1. Taken together, the [1,2,4]triazolo[1,5-*a*]pyrimidine could serve as a promising scaffold for the development of new LSD1 inhibitors.

4. Experimental section

4.1. General Information.

Reagents and solvents were purchased from commercial sources and used without further purification. Thin-layer chromatography (TLC) was carried out on glass plates coated with silica gel (Qingdao Haiyang Chemical Co., G60F-254) and visualized by UV light (254 nm). The products were purified by column chromatography over silica gel (Qingdao Haiyang Chemical Co., 200–300 mesh). Melting points were determined on an X-5 micromelting apparatus and are uncorrected. All the NMR spectra were recorded with a Bruker DPX 400 MHz spectrometer with TMS as internal standard in $CDCl_3$ or DMSO-d_6. Chemical shifts are given as δ ppm values relative to TMS. High-resolution mass spectra (HRMS) were recorded on a Waters Micromass Q-T of Micromass spectrometer by electrospray ionization (ESI).

*4.2. General method for the synthesis of **D1-D22**.*

Compounds **D1-D22** were prepared following the previously reported method [37]. To a solution of 3-amino-5-mercapto-1,2,4-triazole (1.0 g, 8.61 mmol) in acetone (30 mL) were added sodium carbonate (1.37 g, 12.92 mmol), sodium iodide (129.06 mg, 0.861 mmol) and alkyl halide (9.47 mmol). The reaction mixture was stirred at 60 ^{o}C for 3-6 h before cooling to room temperature. Na_2CO_3 and NaI were removed via filtration. The residue was concentrated under vacuum and then dissolved in EtOAc. The organic layer was washed with water (2 × 10 mL) and brine (2 × 20 mL) and then dried over anhydrous $MgSO_4$. After removal of the solvent, the resulting residue was subjected to column chromatography, giving the corresponding products **D1-D22**. Compound **D1**, white solid, yield: 73 %. ^{1}H NMR (400 MHz, DMSO-d_6) δ 7.41-7.18 (m, 5H), 4.34 (s, 2H). ^{13}C NMR (100 MHz, DMSO-d_6) δ 152.19, 147.08, 136.55, 128.79, 128.43, 127.48, 35.41. HRMS (ESI): m/z calcd for $C_9H_9N_4S$ $(M-H)^-$, 205.0548; found, 205.0548.

*4.3. General method for the synthesis of **A1-A29**.*

Compounds **A1-A29** were prepared following the previously reported method [37] as described for **A5**. **D1** (1g, 4.85 mmol) and ethyl acetoacetate (630.94mg, 4.85mmol) was stirred in AcOH (10 mL) at 120 ^{o}C. 3-6 h later, the reaction mixture was cooled to room temperature and the white precipitate formed was filtered and washed using water to afford the desired compound **A5.** Compound **A5**, white solid, yield: 85 %. m.p.: 240-245 ^{o}C. ^{1}H NMR (400 MHz, DMSO-d_6) δ 13.17 (s, 1H), 7.44 (d, J = 7.1 Hz, 2H), 7.32 (t, J = 7.3 Hz, 2H), 7.26 (d, J = 7.2 Hz, 1H), 5.80 (s, 1H), 4.43 (s, 2H), 2.29 (s, 3H). ^{13}C NMR (100MHz, DMSO-d_6) δ 161.92, 154.75, 151.09, 150.63, 137.35, 128.77, 128.38, 127.22, 98.46, 34.48, 18.43. HRMS (ESI): m/z calcd for $C_{13}H_{11}N_4OS$ $(M-H)^-$, 271.0654; found, 271.0660.

*4.4. General method for the synthesis of **B1-B29**.*

Compounds **B1-B29** were prepared following the previously reported method [37] as described for the synthesis of **B5**. **A5** was stirred in $POCl_3$ (excess) at 90 ^{o}C for 3-5h. The resultant oil was added dropwise to ice cold bath. The resulting aqueous mixture was extracted with CH_2Cl_2 (4 × 30 mL) and the organic layers were washed by

saturated aqueous $NaHCO_3$ (3×10 mL). The organic layers were dried over $MgSO_4$ and concentrated under reduced pressure to give the orange solid **B5**, which was used directly without further purification. **B5** was unstable enough and therefore only characterized by HRMS. HRMS (ESI): m/z calcd for $C_{13}H_{12}ClN_4S$ $(M+H)^-$, 291.0471; found, 291.0463.

*4.5. General method for the synthesis of **C1-C32**.*

The general method was described for the synthesis of **C1**. Compound **B1** (150 mg, 0.889 mmol) was dissolved in ethanol (2 mL), followed by addition of the corresponding amine or ammonium hydroxide (0.889 mmol) and triethylamine (180.08 mg, 1.78 mmol) . The reaction mixture was stirred at room temperature for 5 h. The resultant mixture was concentrated under reduced pressure to the residue, which was then purified by column chromatography to give **C1.**

Compound **C1,** white solid, yield: 48 %. m.p.: 162-166 ^oC. ^1H NMR (400 MHz, DMSO-d_6) δ 7.03 (d, J = 8.8 Hz, 2H), 6.94 (d, J = 8.9 Hz, 2H), 5.84 (s, 1H), 3.16 – 3.06 (m, 5H), 2.48 – 2.41 (m, 4H), 2.22 (d, J = 3.5 Hz, 6H). ^{13}C NMR (100 MHz, DMSO-d_6) δ 161.34, 156.47, 152.96, 147.82, 124.56, 116.28, 88.26, 54.69, 48.55, 45.74, 24.48. HRMS (ESI): m/z calcd for $C_{17}H_{22}N_7$ $(M+H)^+$, 324.1936; found, 324.1907.

Compound **C2,** white solid, yield: 61 %. m.p.: 153-156 ^oC. ^1H NMR (400 MHz, DMSO-d_6) δ 8.48 (s, 1H), 7.27 (d, J = 8.7 Hz, 2H), 7.03 (d, J = 8.6 Hz, 2H), 6.17 (s, 1H), 3.19 (s, 4H), 2.66 (dd, J = 14.8, 7.3 Hz, 2H), 2.26 (s, 3H), 1.18 (t, J = 7.5 Hz, 3H). ^{13}C NMR (100 MHz, DMSO-d_6) δ 154.34, 125.88, 115.85, 54.43, 47.80, 45.56, 30.97, 12.98. HRMS (ESI): m/z calcd for $C_{18}H_{24}N_7$ $(M+H)^+$, 338.2093; found, 338.2059.

Compound **C3,** white solid, yield: 58 %. m.p.: 176-179 ^oC. ^1H NMR (400 MHz, DMSO-d_6) δ 8.59 (s, 1H), 7.99 (dd, J = 6.4, 2.9 Hz, 2H), 7.58 – 7.47 (m, 3H), 7.43 (d, J = 8.8 Hz, 2H), 7.14 (d, J = 8.8 Hz, 2H), 6.74 (s, 1H), 3.87 (s, 2H), 3.47 (s, 2H), 3.17 (s, 4H), 2.82 (s, 3H). ^{13}C NMR (100 MHz, DMSO-d_6) δ 160.48, 155.88, 155.01, 147.94, 147.15, 137.45, 130.35, 128.80, 128.56, 127.13, 125.88, 116.64, 85.68, 55.99,

52.06, 45.36, 41.94, 18.52. HRMS (ESI): m/z calcd for $C_{22}H_{24}N_7$ $(M+H)^+$, 386.2093; found, 386.2092.

Compound **C4,** white solid, yield: 65 %. m.p.: 137-142 ^oC. ^1H NMR (400 MHz, DMSO-d_6) δ 7.14 (d, *J* = 8.7 Hz, 2H), 6.95 (d, *J* = 8.8 Hz, 2H), 3.22 – 3.08 (m, 4H), 2.80 (t, *J* = 7.7 Hz, 2H), 2.49 – 2.41 (m, 4H), 2.23 (s, 3H), 2.14 (t, *J* = 7.2 Hz, 2H), 1.98 – 1.80 (m, 2H). ^{13}C NMR (100 MHz, DMSO-d_6) δ 173.08, 155.62, 153.81, 149.55, 146.34, 142.51, 127.93, 127.68, 114.77, 102.24, 55.99, 54.52, 47.88, 45.69, 34.09, 30.66, 28.46, 22.95, 18.52.

HRMS (ESI): m/z calcd for $C_{19}H_{24}N_7$ $(M+H)^+$, 350.2093; found, 350.2064.

Compound **C5,** white solid, yield: 52 %. m.p.: 155-158 ^oC. ^1H NMR (400 MHz, DMSO-d_6) δ 7.49 (d, *J* = 7.3 Hz, 2H), 7.30 (m, 5H), 7.10 (d, *J* = 8.9 Hz, 2H), 6.15 (s, 1H), 4.55 (s, 2H), 3.84 (s, 2H), 3.60 – 3.43 (m, 2H), 3.19 (d, *J* = 9.8 Hz, 4H), 2.81 (s, 3H), 2.36 (s, 3H). ^{13}C NMR (100 MHz, DMSO-d_6) δ 164.43, 163.68, 155.77, 147.98, 145.57, 138.02, 128.90, 128.50, 128.42, 127.20, 126.03, 116.61, 88.93, 51.99, 45.36, 41.89, 34.50, 24.63. HRMS (ESI): m/z calcd for $C_{24}H_{28}N_7S$ $(M+H)^+$, 446.2126; found, 446.2094.

Compound **C6,** white solid, yield: 43 %. m.p.: 182-184 ^oC. ^1H NMR (400 MHz, DMSO-d_6) δ 7.52 (d, *J* = 8.4 Hz, 2H), 7.37 (d, *J* = 8.4 Hz, 2H), 7.30 (d, *J* = 8.8 Hz, 2H), 7.10 (d, *J* = 8.9 Hz, 2H), 6.14 (s, 1H), 4.52 (s, 2H), 2.81 (s, 3H), 2.35 (s, 3H). ^{13}C NMR (100 MHz, DMSO-d_6) δ 164.14, 163.76, 155.77, 148.00, 145.55, 137.43, 131.78, 130.78, 128.44, 128.33, 126.05, 116.61, 88.96, 52.07, 45.43, 41.98, 33.58, 24.62. HRMS (ESI): m/z calcd for $C_{24}H_{27}FN_7S$ $(M+H)^+$, 464.2032; found, 464.1995.

Compound **C7,** white solid, yield: 58 %. m.p.: 172-175 ^oC. ^1H NMR (400 MHz, DMSO-d_6) δ 7.54 (dd, *J* = 8.6, 5.6 Hz, 2H), 7.30 (d, *J* = 8.9 Hz, 2H), 7.19 – 7.06 (m, 4H), 6.14 (s, 1H), 4.53 (s, 2H), 2.82 (s, 3H), 2.36 (s, 3H). ^{13}C NMR (100 MHz, DMSO-d_6) δ 164.27, 163.74, 160.10, 155.77, 147.98, 145.55, 134.49, 130.95, 130.87, 128.47, 126.03, 116.62, 115.26, 115.05, 88.94, 52.10, 45.45, 42.00, 33.56, 24.63. HRMS (ESI): m/z calcd for $C_{24}H_{27}ClN_7S$ $(M+H)^+$, 480.1737; found, 480.1697.

Compound **C8,** white solid, yield: 62 %. m.p.: 162-165 ^oC. ^1H NMR (400 MHz, DMSO-d_6) δ 7.48 (q, *J* = 8.5 Hz, 4H), 7.30 (d, *J* = 8.8 Hz, 2H), 7.09 (d, *J* = 8.9 Hz,

2H), 6.14 (s, 1H), 4.51 (s, 2H), 3.27 (s, 8H), 2.77 (s, 3H), 2.35 (s, 3H). ^{13}C NMR (100 MHz, DMSO-d_6) δ 164.12, 163.74, 155.77, 148.09, 145.57, 137.86, 131.24, 131.13, 128.37, 126.04, 120.29, 116.56, 88.95, 52.20, 45.55, 42.18, 33.66, 24.63. HRMS (ESI): m/z calcd for $C_{24}H_{27}BrN_7S$ $(M+H)^+$, 524.1232; found, 524.1182.

Compound **C9,** white solid, yield: 41 %. m.p.: 142-146 ^{o}C. ^{1}H NMR (400 MHz, DMSO-d_6) δ 7.72 (d, *J* = 6.6 Hz, 1H), 7.65 (d, *J* = 7.8 Hz, 1H), 7.33 (dd, *J* = 14.9, 8.0 Hz, 3H), 7.23 (t, *J* = 7.0 Hz, 1H), 7.10 (d, *J* = 8.8 Hz, 2H), 6.15 (s, 1H), 4.62 (s, 2H), 2.80 (s, 3H), 2.36 (s, 3H). ^{13}C NMR (100 MHz, DMSO-d_6) δ 164.00, 163.79, 155.80, 148.03, 145.59, 136.92, 132.72, 131.42, 129.59, 128.43, 127.90, 126.06, 124.02, 116.60, 89.00, 52.05, 45.41, 41.97, 35.23, 24.64. HRMS (ESI): m/z calcd for $C_{24}H_{27}BrN_7S$ $(M+H)^+$, 524.1232; found, 524.1192.

Compound **C10,** white solid, yield: 59 %. m.p.: 163-169 ^{o}C. ^{1}H NMR (400 MHz, DMSO-d_6) δ 7.80 (s, 1H), 7.57 (d, *J* = 7.7 Hz, 1H), 7.53 – 7.47 (m, 1H), 7.34 (d, *J* = 7.8 Hz, 1H), 7.32 – 7.26 (m, 2H), 7.07 (d, *J* = 9.0 Hz, 2H), 6.17 (s, 1H), 4.58 (s, 2H), 3.29 – 3.18 (m, 4H), 2.54 – 2.49 (m, 4H), 2.40 (s, 3H), 2.28 (s, 3H). ^{13}C NMR (100 MHz, DMSO-d_6) δ 163.99, 163.70, 155.80, 149.47, 145.68, 141.25, 131.63, 130.53, 130.01, 128.03, 127.20, 126.02, 121.43, 115.79, 88.89, 54.53, 47.89, 45.72, 33.57, 24.62. HRMS (ESI): m/z calcd for $C_{24}H_{27}BrN_7S$ $(M+H)^+$, 524.1232; found, 524.1192.

Compound **C11,** white solid, yield: 86 %. m.p.: 172-175 ^{o}C. ^{1}H NMR (400 MHz, DMSO-d_6) δ 8.18 (d, *J* = 8.7 Hz, 2H), 7.79 (d, *J* = 8.7 Hz, 2H), 7.27 (d, *J* = 8.8 Hz, 2H), 7.07 (d, *J* = 8.9 Hz, 2H), 6.13 (s, 1H), 4.65 (s, 2H), 3.35 (s, 4H), 2.96 (s, 4H), 2.58 (s, 3H), 2.35 (s, 3H). ^{13}C NMR (100 MHz, DMSO-d_6) δ 163.75, 155.79, 148.63, 146.69, 146.55, 145.64, 130.17, 127.88, 126.06, 124.50, 123.48, 116.27, 88.99, 53.13, 46.48, 33.54, 24.61. HRMS (ESI): m/z calcd for $C_{24}H_{27}N_8O_2S$ $(M+H)^+$, 491.1977; found, 491.1933.

Compound **C12,** white solid, yield: 76 %. m.p.: 167-175 ^{o}C. ^{1}H NMR (400 MHz, DMSO-d_6) δ 8.13 – 8.04 (m, 1H), 7.92 (d, *J* = 7.7 Hz, 1H), 7.71 (m, 1H), 7.62 – 7.51 (m, 1H), 7.31 (d, *J* = 8.9 Hz, 2H), 7.10 (d, *J* = 8.9 Hz, 2H), 6.15 (s, 1H), 4.83 (s, 2H), 3.49 (s, 8H), 2.77 (s, 3H), 2.36 (s, 3H). ^{13}C NMR (100 MHz, DMSO-d_6) δ 163.97, 163.83, 155.78, 148.15, 147.93, 145.59, 133.90, 133.63, 132.50, 129.01, 128.30,

126.07, 124.99, 116.55, 89.03, 52.20, 45.56, 42.20, 31.79, 24.62. HRMS (ESI): m/z calcd for $C_{24}H_{27}N_8O_2S$ $(M+H)^+$, 491.1977; found, 491.1929.

Compound **C13,** white solid, yield: 76 %. m.p.: 161-165 ^oC. ^1H NMR (400 MHz, DMSO-d_6) δ 7.41 (d, J = 8.7 Hz, 2H), 7.30 (d, J = 8.9 Hz, 2H), 7.10 (d, J = 9.0 Hz, 2H), 6.88 (d, J = 8.7 Hz, 2H), 6.14 (s, 1H), 4.48 (s, 2H), 3.72 (s, 4H), 2.82 (s, 3H), 2.36 (s, 3H). ^{13}C NMR (100 MHz, DMSO-d_6) δ 164.56, 163.68, 158.46, 155.77, 147.95, 145.53, 130.13, 129.72, 128.52, 126.01, 116.63, 113.83, 55.04, 52.12, 45.47, 34.06, 24.64. HRMS (ESI): m/z calcd for $C_{25}H_{30}N_7OS$ $(M+H)^+$, 476.2232; found, 476.2190.

Compound **C14,** white solid, yield: 59 %. m.p.: 158-167 ^oC. ^1H NMR (400 MHz, DMSO-d_6) δ 7.60 (dd, J = 10.5, 1.7 Hz, 1H), 7.53 (t, J = 8.1 Hz, 1H), 7.42 – 7.36 (m, 1H), 7.29 (d, J = 8.8 Hz, 2H), 7.09 (d, J = 8.8 Hz, 2H), 6.14 (s, 1H), 4.53 (s, 2H), 3.19 (s, 8H), 2.73 (s, 3H), 2.36 (s, 3H). ^{13}C NMR (100 MHz, DMSO-d_6) δ 163.91, 155.79, 148.23, 145.60, 140.39, 130.46, 126.07, 124.51, 117.42, 116.51, 88.98, 52.51, 45.84, 33.22, 24.62. HRMS (ESI): m/z calcd for $C_{24}H_{26}ClFN_7S$ $(M+H)^+$, 498.1643; found, 498.1597.

Compound **C15,** white solid, yield: 67 %. m.p.: 172-175 ^oC. ^1H NMR (400 MHz, DMSO-d_6) δ 7.78 (dd, J = 7.2, 2.1 Hz, 1H), 7.58 – 7.48 (m, 1H), 7.41 – 7.26 (m, 3H), 7.10 (d, J = 8.9 Hz, 2H), 6.14 (s, 1H), 4.52 (s, 2H), 3.21 (s, 8H), 2.74 (s, 3H), 2.36 (s, 3H). ^{13}C NMR (100 MHz, DMSO-d_6) δ 163.97, 163.78, 157.55, 155.80, 155.10, 148.22, 145.59, 136.55, 130.98, 129.69, 129.62, 128.26, 126.08, 119.12, 116.86, 116.66, 116.51, 88.96, 52.39, 45.74, 42.46, 32.99, 24.63. HRMS (ESI): m/z calcd for $C_{24}H_{26}ClFN_7S$ $(M+H)^+$, 498.1643; found, 498.1600.

Compound **C16,** white solid, yield: 66 %. m.p.: 191-196 ^oC. ^1H NMR (400 MHz, DMSO-d_6) δ 7.54 (d, J = 8.1 Hz, 2H), 7.44 – 7.36 (m, 1H), 7.25 (d, J = 8.9 Hz, 2H), 7.02 (d, J = 9.0 Hz, 2H), 6.15 (s, 1H), 5.76 (s, 1H), 4.83 (s, 2H), 3.20 – 3.12 (m, 4H), 2.49 – 2.44 (m, 4H), 2.37 (s, 3H), 2.23 (s, 3H). ^{13}C NMR (100 MHz, DMSO-d_6) δ 163.80, 155.81, 149.41, 145.74, 135.09, 132.23, 130.45, 128.79, 127.23, 125.92, 115.78, 89.00, 59.72, 54.87, 54.52, 47.88, 45.69, 31.49, 24.66, 20.72, 14.05. HRMS (ESI): m/z calcd for $C_{24}H_{26}Cl_2N_7S$ $(M+H)^+$, 514.1347; found, 514.1304.

Compound **C17,** white solid, yield: 75 %. m.p.: 188-192 °C. ^{1}H NMR (400 MHz, DMSO-d_6) δ 7.36 (d, J = 8.0 Hz, 2H), 7.24 (d, J = 8.9 Hz, 2H), 7.12 (d, J = 7.9 Hz, 2H), 7.01 (d, J = 9.0 Hz, 2H), 6.11 (s, 1H), 4.49 (s, 2H), 3.21 – 3.11 (m, 4H), 2.49 – 2.43 (m, 4H), 2.35 (s, 3H), 2.26 (s, 3H), 2.23 (s, 3H). ^{13}C NMR (100 MHz, DMSO-d_6) δ 164.45, 163.61, 155.78, 149.42, 145.64, 136.40, 134.82, 128.97, 128.82, 127.23, 125.97, 115.78, 88.81, 54.52, 47.88, 45.69, 34.29, 24.62, 20.65. HRMS (ESI): m/z calcd for $C_{25}H_{30}N_7S$ $(M+H)^+$, 460.2283; found, 460.2260.

Compound **C18,** white solid, yield: 67 %. m.p.: 172-176 °C. ^{1}H NMR (400 MHz, DMSO-d_6) δ 7.71 (dd, J = 23.9, 8.2 Hz, 4H), 7.30 (d, J = 8.8 Hz, 2H), 7.10 (d, J = 8.9 Hz, 2H), 6.14 (s, 1H), 4.62 (s, 2H), 2.81 (s, 3H), 2.35 (s, 3H). ^{13}C NMR (100 MHz, DMSO-d_6) δ 163.98, 163.78, 155.79, 148.03, 145.59, 143.41, 129.69, 128.43, 127.87, 127.56, 126.06, 125.24, 125.20, 122.86, 116.60, 88.99, 52.05, 45.40, 41.96, 33.72, 24.61. HRMS (ESI): m/z calcd for $C_{25}H_{27}F_3N_7S$ $(M+H)^+$, 514.2000; found, 514.1956.

Compound **C19,** white solid, yield: 58 %. m.p.: 161-165 °C. ^{1}H NMR (400 MHz, DMSO-d_6) δ 7.31 (t, J = 4.3 Hz, 6H), 7.27 – 7.21 (m, 1H), 7.10 (d, J = 8.4 Hz, 2H), 6.13 (s, 1H), 3.67 – 3.48 (m, 10H), 3.05 (t, J = 7.5 Hz, 2H), 2.81 (s, 3H), 2.36 (s, 3H). ^{13}C NMR (100 MHz, DMSO-d_6) δ 164.68, 163.60, 155.83, 147.99, 145.57, 140.00, 128.62, 128.52, 128.32, 126.31, 126.07, 116.62, 88.87, 52.12, 45.47, 42.03, 35.43, 31.88, 24.61. HRMS (ESI): m/z calcd for $C_{25}H_{30}N_7S$ $(M+H)^+$, 460.2283; found, 460.2242.

Compound **C20,** white solid, yield: 77 %. m.p.: 152-156 °C. ^{1}H NMR (400 MHz, DMSO-d_6) δ 7.24 (m, 7H), 7.01 (d, J = 9.0 Hz, 2H), 6.10 (s, 1H), 3.25 (t, J = 7.1 Hz, 2H), 3.20 – 3.11 (m, 4H), 2.82 – 2.69 (m, 2H), 2.50 – 2.43 (m, 4H), 2.34 (s, 3H), 2.23 (s, 3H), 2.05 (m, 2H). ^{13}C NMR (100 MHz, DMSO-d_6) δ 164.68, 163.48, 155.80, 149.41, 145.65, 141.16, 128.32, 128.30, 127.27, 126.01, 125.84, 115.78, 88.76, 54.52, 47.88, 45.69, 33.99, 31.12, 30.20, 24.61. HRMS (ESI): m/z calcd for **C26**$H_{32}N_7S$ $(M+H)^+$, 474.2439; found, 474.2399.

Compound **C21,** white solid, yield: 73 %. m.p.: 192-197 °C. ^{1}H NMR (400 MHz, DMSO-d_6) δ 7.23 (d, J = 8.9 Hz, 2H), 7.02 (d, J = 9.0 Hz, 2H), 6.09 (s, 1H), 3.27 – 3.20 (m, 2H), 3.19 – 3.13 (m, 5H), 2.46 (d, J = 4.9 Hz, 4H), 2.34 (s, 3H), 2.23 (s, 3H),

1.75 (dd, *J* = 14.4, 7.2 Hz, 2H), 1.01 (t, *J* = 7.3 Hz, 3H). ^{13}C NMR (100 MHz, DMSO-d_6) δ 155.80, 155.22, 126.03, 117.13, 115.78, 54.54, 47.90, 32.51, 24.61, 22.84, 13.07. HRMS (ESI): m/z calcd for $C_{20}H_{28}N_7S$ $(M+H)^+$, 398.2126; found, 398.2094.

Compound **C22,** white solid, yield: 62 %. m.p.: 162-165 °C. ^{1}H NMR (400 MHz, DMSO-d_6) δ 7.24 (d, *J* = 8.9 Hz, 2H), 7.02 (d, *J* = 9.0 Hz, 2H), 6.11 (s, 1H), 6.08 – 5.97 (m, 1H), 5.36 (dd, *J* = 16.9, 1.5 Hz, 1H), 5.13 (d, *J* = 10.0 Hz, 1H), 3.94 (d, *J* = 6.9 Hz, 2H), 3.23 – 3.11 (m, 4H), 2.49 – 2.43 (m, 4H), 2.35 (s, 3H), 2.23 (s, 3H). ^{13}C NMR (100 MHz, DMSO-d_6) δ 164.15, 163.60, 155.82, 149.44, 145.67, 134.00, 127.23, 126.00, 118.02, 115.77, 88.79, 54.54, 47.90, 45.72, 33.25, 24.62. HRMS (ESI): m/z calcd for $C_{20}H_{26}N_7S$ $(M+H)^+$, 396.1970; found, 396.1935.

Compound **C23,** white solid, yield: 72 %. m.p.: 202-205 °C. ^{1}H NMR (400 MHz, DMSO-d_6) δ7.31 (d, *J* = 8.8 Hz, 2H), 7.10 (d, *J* = 8.9 Hz, 2H), 6.16 (s, 1H), 4.13 (d, *J* = 2.5 Hz, 2H), 3.23 (t, *J* = 2.5 Hz, 1H), 2.81 (s, 3H), 2.36 (s, 3H). ^{13}C NMR (100 MHz, DMSO-d_6) δ 163.89, 163.27, 155.82, 147.98, 145.63, 128.44, 125.98, 116.62, 89.07, 80.18, 73.90, 52.05, 45.40, 41.95, 24.66, 19.11, 18.50. HRMS (ESI): m/z calcd for $C_{20}H_{24}N_7S$ $(M+H)^+$, 394.1813; found, 394.1777.

Compound **C24,** white solid, yield: 38 %. m.p.: 158-165 °C. ^{1}H NMR (400 MHz, DMSO-d_6) δ 6.99 (d, *J* = 8.7 Hz, 2H), 6.78 (d, *J* = 8.8 Hz, 2H), 5.81 (s, 1H), 2.90 (d, *J* = 7.2 Hz, 4H), 2.20 (s, 1H), 2.03 (s, 3H), 0.92 (m, 1H), 0.33 – 0.19 (m, 2H), 0.02 (d, *J* = 4.9 Hz, 2H). ^{13}C NMR (100 MHz, DMSO-d_6) δ 165.04, 163.53, 155.77, 147.97, 145.50, 128.50, 126.02, 116.57, 88.79, 51.98, 45.34, 41.89, 36.19, 24.62, 11.22, 5.64. HRMS (ESI): m/z calcd for $C_{21}H_{28}N_7S$ $(M+H)^+$, 410.2126; found, 410.2093.

Compound **C25,** white solid, yield: 68 %. m.p.: 198-204 °C. ^{1}H NMR (400 MHz, DMSO-d_6) δ 7.27 (d, *J* = 8.8 Hz, 2H), 7.07 (d, *J* = 8.9 Hz, 2H), 6.11 (s, 1H), 3.18 (d, *J* = 6.8 Hz, 3H), 2.98 (d, *J* = 4.9 Hz, 5H), 2.58 (s, 3H), 2.35 (s, 3H), 1.85 (d, *J* = 12.2 Hz, 2H), 1.65 (dd, *J* = 29.6, 10.5 Hz, 4H), 1.28 – 0.95 (m, 7H). ^{13}C NMR (100 MHz, DMSO-d_6) δ 165.14, 163.48, 155.72, 145.55, 128.65, 128.27, 128.01, 126.04, 116.26, 114.37, 88.77, 53.14, 46.38, 33.14, 31.81, 25.81, 25.43, 24.61. HRMS (ESI): m/z calcd for $C_{24}H_{34}N_7S$ $(M+H)^+$, 452.2596; found, 452.2554.

Compound **C26,** white solid, yield: 83 %. m.p.: 168-172 ^{o}C. ^{1}H NMR (400 MHz, DMSO-d_6) δ 7.77 (dd, *J* = 6.0, 3.1 Hz, 2H), 7.50 (dd, *J* = 6.1, 3.1 Hz, 2H), 7.36 (d, *J* = 8.7 Hz, 2H), 7.13 (d, *J* = 8.8 Hz, 2H), 6.17 (s, 1H), 5.03 (s, 2H), 3.87 (s, 2H), 3.51 (s, 2H), 3.19 (s, 4H), 2.83 (s, 3H), 2.34 (s, 3H). ^{13}C NMR (100 MHz, DMSO-d_6) δ 163.80, 162.68, 155.85, 150.89, 148.12, 145.69, 131.74, 128.16, 126.26, 125.37, 116.58, 114.07, 89.18, 51.98, 45.33, 41.87, 25.57, 24.43. HRMS (ESI): m/z calcd for $C_{25}H_{28}N_9S$ $(M+H)^+$, 486.2188; found, 486.2148.

Compound **C27,** white solid, yield: 78 %. m.p.: 156-161 ^{o}C. ^{1}H NMR (400 MHz, DMSO-d_6) δ 8.10 (d, *J* = 1.8 Hz, 1H), 8.03 (d, *J* = 8.6 Hz, 1H), 7.95 (s, 1H), 7.42 (dd, *J* = 8.6, 1.8 Hz, 1H), 7.31 (d, *J* = 8.8 Hz, 2H), 7.10 (d, *J* = 8.9 Hz, 2H), 6.15 (s, 1H), 4.82 (s, 2H), 3.47 (s, 8H), 2.81 (s, 3H), 2.36 (s, 3H). ^{13}C NMR (100 MHz, DMSO-d_6) δ 164.17, 163.79, 155.85, 148.04, 145.61, 139.13, 138.23, 131.52, 129.50, 128.43, 126.10, 124.71, 124.54, 121.65, 116.60, 88.94, 52.10, 45.45, 42.01, 27.75, 24.65. HRMS (ESI): m/z calcd for **C26**$H_{27}ClN_7S_2$ $(M+H)^+$, 536.1457; found, 536.1411.

Compound **C28,** white solid, yield: 82 %. m.p.: 210-215 ^{o}C. ^{1}H NMR (400 MHz, DMSO-d_6) δ 7.42 (d, *J* = 8.4 Hz, 2H), 7.33 (d, *J* = 8.4 Hz, 2H), 6.98 (d, *J* = 8.9 Hz, 2H), 6.91 (d, *J* = 9.0 Hz, 2H), 4.41 (s, 2H), 3.16 – 3.08 (m, 4H), 2.49 – 2.44 (m, 4H), 2.43 (s, 3H), 2.22 (s, 3H), 1.80 (s, 3H). ^{13}C NMR (100 MHz, DMSO-d_6) δ 163.85, 163.33, 154.22, 148.12, 142.47, 137.44, 131.71, 130.76, 130.64, 128.24, 124.09, 115.31, 101.08, 54.47, 48.14, 45.59, 33.52, 23.83, 13.67. HRMS (ESI): m/z calcd for $C_{25}H_{29}ClN_7S$ $(M+H)^+$, 494.1893; found, 494.1849.

Compound **C29,** white solid, yield: 67 %. m.p.: 169-173 ^{o}C. ^{1}H NMR (400 MHz, DMSO-d_6) δ 7.33 (dd, *J* = 19.6, 8.4 Hz, 4H), 7.02 (d, *J* = 8.7 Hz, 2H), 6.91 (d, *J* = 8.8 Hz, 2H), 4.33 (s, 2H), 3.10 (s, 4H), 2.46 (s, 6H), 2.40 – 2.32 (m, 2H), 2.22 (s, 3H), 1.33 – 1.19 (m, 3H), 1.13 (m, 2H), 1.05 – 0.95 (m, 2H), 0.76 (t, *J* = 7.2 Hz, 3H). ^{13}C NMR (100 MHz, DMSO-d_6) δ 163.38, 163.10, 154.24, 148.73, 142.86, 137.48, 131.67, 130.75, 130.22, 128.19, 125.53, 115.26, 105.88, 54.87, 54.33, 48.16, 45.49, 33.40, 31.10, 28.03, 25.64, 23.34, 21.80, 13.90. HRMS (ESI): m/z calcd for $C_{29}H_{37}ClN_7S$ $(M+H)^+$, 550.2519; found, 550.2471.

Compound **C30**, white solid, yield: 85 %. m.p.: 189-192 ^{o}C . ^{1}H NMR (400 MHz, $CDCl_3$) δ 7.71 (s, 1H), 7.51-7.44 (m, 4H), 7.36-7.27 (m, 5H), 7.26-7.20 (m, 1H), 6.30 (s, 1H), 4.54 (s, 2H), 2.51 (s, 3H). ^{13}C NMR (100 MHz, $CDCl_3$) δ 166.54, 164.77, 155.92, 144.35, 137.57, 135.76, 130.02, 129.11, 128.53, 127.36, 126.92, 123.82, 89.01, 35.80, 25.41. HRMS (ESI): m/z calcd for $C_{19}H_{16}N_5S$ $(M-H)^-$, 346.1126; found, 346.1135.

Compound **C31**, yellow solid, yield: 89 %. m.p.: 196-201 ^{o}C. ^{1}H NMR (400 MHz, DMSO-d_6) δ 7.93 (s, 2H), 7.55-7.43 (m, 2H), 7.37-7.28 (m, 2H), 7.24 (dd, J = 8.4, 6.1 Hz, 1H), 6.12 (s, 1H), 4.49 (s, 2H), 2.37 (s, 3H). ^{13}C NMR (100 MHz, DMSO-d_6) δ 164.29, 162.84, 155.87, 147.50, 138.07, 128.92, 128.38, 127.16, 90.25, 34.36, 24.37. HRMS (ESI): m/z calcd for $C_{13}H_{12}N_5S$ $(M-H)^-$, 270.0813; found, 270.0821.

Compound **C32**, white solid, yield: 79%. m.p.: 180-19 ^{o}C. 1H NMR (400 MHz, DMSO-d_6) δ 10.15 (s, 1H), 7.50 (m, 6H), 7.33 (d, J = 7.0 Hz, 1H), 7.18 (dd, J = 6.0, 3.1 Hz, 2H), 6.34 (s, 1H), 4.79 (s, 2H), 2.38 (s, 3H). 13C NMR (100 MHz, DMSO-d_6) δ 164.03, 163.80, 155.80, 150.66, 144.94, 136.53, 129.48, 126.12, 124.44, 122.01, 114.75, 89.29, 28.00, 24.60. HRMS (ESI): m/z calcd for $C_{20}H_{16}N_7S$ $(M-H)^-$, 386.1188; found, 386.1196.

4.6. Cell proliferation assay

The MTT assay was carried out following our previously reported methods [58] to evaluate the antiproliferative activity of **C26**.

4.7. LSD1 enzymatic assay

Full length LSD1 cDNA encoding LSD1 was obtained by RT-PCR and cloned into pET-28b (pET-28b-LSD1). Then the plasmid pET-28b-LSD1 was transfected into BL21 (DE). The recombinant protein was induced with 0.25 mM IPTG at 20 ^{o}C and purified following affinity chromatography, ion exchange chromatography and gel filtration. Then the compounds were incubated with the 5 nM recombinant LSD1 and 25 μM H3K4me2 peptide in the present of FAD (50 nM), Amplex Red (20 nM) and horseradish peroxidase (5.5 U/mL) for 30 min. After that, the fluorescence was measured at excitation wavelength 530 nm and emission wavelength 590 nm as reported in order to evaluate the inhibition rate of the candidate compounds.

4.8. HRP enzymatic assay

The HRP enzymatic assay was performed using a catalase activity test kit (Catalase Assay Kit, Beyotime). Compound **C26** or DMSO was incubated with HRP for 10 min. Then, the above mixture (10 μL) was transferred into a tube with 10 μL H_2O_2 (250 mM) and 30 μL reaction buffer in the kit. The system was mixed quickly and incubated at 25 □ for 3 min, followed by addition of stop buffer (450 μL). Finally, 2 μL of mixture was transferred from the tube to the 96-well plate which contains 8 μL of reaction buffer and 200 μL of working buffer, the mixture was then incubated for 20 min, followed by absorbance measurement at 520 nm.

4.9. Hydrogen peroxide (H2O2) measurement

The hydrogen peroxide quantitation assay was carried out by the ferrous ion oxidation-xylenol orange (FOX) method [23]. A sample of PBS (50 μL) was mixed with different concentrations of compound **C26** or **C32**. Then, the FOX reagent (100 μL) was added, followed by shaking and additional incubation for 30 min. The absorbance at 560 nm was read against a DMSO blank.

4.10. MAO-A and MAO-B enzymatic assay

The MAO-A/B were purchased from Active Motif (Cat#31502, Cat#31503). Biochemical Kits were purchased from Promega (MAO-Glo Assay, V1402). Inhibition assay was carried out according to the manufacturer's protocol. The tested compound solution was transferred into a 384-well plate by Echo 550 in duplicate, then incubated with 10 μL of recombinant MAO-A or MAO-B solutions at room temperature for 15 min (the final concentration was 15 and 20 nM, respectively), followed by adding 10 μL of luciferin derivative substrate (the final concentration is 10 uM respectively) to initiate the reaction. After incubation for 60 min at room temperature, the reporter luciferase detection reagent (20 μL) was added and incubated with each reaction for an additional 20 min. Relative light units (RLU) were detected using EnVision Multilabel Plate Reader.

4.11. Reversible assay

The dilution assay was done as published. Briefly, an amount of 2.5 μg of LSD1 recombinant was incubated with compound **C26** (40 μM), 1.6 μM GSK2879552，or DMSO. At 1h later, 1.25 μL aliquots were removed from all samples and diluted into HRP-assay solution containing substrate and coupling reagents to a final volume of

100 μL.

4.12. Competitive assay

For the competitive analysis of compound **C26**, the demethylase activity of LSD1 was assessed in the presence of different concentrations of the compound (0, 0.625, 1.25, and 2.5 μM) at a fixed concentration of FAD (2.5 μM) and peptide concentrations from 0.8 to 106 μM or fixed concentration of peptide (10 μM) and FAD concentrations from 1 to 128 μM. Assays were performed triplicate, and kinetics values were obtained using Lineweaver-Burk plots.

4.13. Molecular docking studies

All molecular modeling studies were performed with the Molecular Operating Environment software (MOE 2014.09 version). The crystal structure of LSD1 (PDB code: 2v1d) was downloaded from the RCSB protein database [57], followed by water molecule deletion, structure correction and protonation using the default structure preparation module. Energy minimization was then performed using the Amber 10: EHT forcefield. The structure of compound **C26** was generated with ChemDraw and then pasted into the MOE window for protonation, energy minimization and conformational search. The generated conformations were then docked into the ligand binding sites of LSD1 using the default DOCK module. The conformation was scored by London dG and GBVI/WSA dG.

4.14. Transwell assay

For the migration assay, 400 μL medium without FBS, different concentrations of compound **C26** and 8000 cells were added to each upper chamber. In the lower chamber, 600 μL medium with 20% FBS was used as chemoattractant. After incubation for 48 h, both chambers were washed by PBS for three times. After staining with Hoechst33258 (10 μg/mL) and twice wash, migrated cells were detected and numbered using high content screening system (ArrayScan XTI, Thermo Fisher Scientific, MA).

4.15. Cellular thermal shift assay.

Briefly, cells (5×10^5 per sample) were treated with **C26** or with DMSO for 1 h, washed with PBS three times, and dissolved in 50 μL PBS supplemented with a

protease inhibitor, followed by heating at the indicated temperatures. Treated cells were then subjected to snap-freezing in liquid nitrogen and thawed on ice for 3 cycles. The protein levels of LSD1 in equal amounts of the supernatant were examined by western blots. GAPDH was used as the control. Results are representative of three independent experiments.

4.16. Western blot assay

Cells were seeded and treated with 0, 8, and 16 μM of compound **C26** for 24 h, then cells were collected and lysed by radio immunoprecipitation assay (RIPA) lysis buffer (50 mM Tris-HCl, pH 7.5, 150 mM NaCl, 0.25% sodium deoxycholate, 0.1% Nonidet P-40, 0.1% Triton X-100) with the complete proteinase inhibitor cocktail (Roche, Basel, Switzerland) for 30 min. After centrifugation of 12,000 rpm for 10 min at 4 rpm for centrifugation of 1r cocktail (Roche, Basel, Switzerland) for l, pH 7.5,bicinchonininc acid (BCA) assay kit (Beyotmie Biotechnology, Haimen, China). After added with loading buffer, cell lyses were boiled for 10 min at 100fer, cell lyses were mide gel electrophoresis (PAGE). Proteins were transferred to nitrocellulose (NC) membranes. The membranes were blocked with 5% skim milk at room temperature for 2 h, and then incubated overnight at 4nd with primary antibodies. After washing the membrane with TBST (TBS, 0.05% Tween-20) /TBS three times (5 min per wash), blots were incubated with the secondary antibody (1:5000) at room temperature for 2 h. Finally, the blots were washed in TBST/TBS. The antibody-reactive bands were revealed by enhanced chemiluminescence (ECL) and exposed on Kodak radiographic film.

Acknowledgment

This work was supported by the National Natural Science Foundation of China (No. 81430085, 81773562 and 81703326), the open fund of state key laboratory of Pharmaceutical Biotechnology, Nan-jing University, China (Grant no. KF-GN-201902), Scientific Program of Henan Province (No. 182102310123), China Postdoctoral Science Foundation (No. 2018M630840), Key Research Program of Higher Education of Henan Province (No. 18B350009), and the Starting Grant of Zhengzhou University (No. 32210533).

References

1. Shi Y.; Lan F.; Matson C.; Mulligan P.; Whetstine J. R.; Cole P. A.; Casero R. A.; Shi Y. Histone Demethylation Mediated by the Nuclear Amine Oxidase Homolog LSD1. *Cell* 119 (**2004**) 941-953.

2. Forneris F.; Binda C.; Vanoni M. A.; Mattevi A.; Battaglioli E. Histone demethylation catalysed by LSD1 is a flavin-dependent oxidative process. *FEBS Letters* 579 (**2005**) 2203-2207.

3. Fu X.; Zhang P.; Yu B. Advances toward LSD1 inhibitors for cancer therapy. *Future Medicinal Chemistry* 9 (**2017**) 1227-1242.

4. Maiques-Diaz A., CP Somervaille T. LSD1: biologic roles and therapeutic targeting. Epigenomics 8 (**2016**) 1103-1116.

5. Hayami S.; Kelly J. D.; Cho H. S.; Yoshimatsu M.; Unoki M.; Tsunoda T.; Field H. I.; Neal D. E.; Yamaue H.; Ponder B. A.; Nakamura Y.; Hamamoto R. Overexpression of LSD1 contributes to human carcinogenesis through chromatin regulation in various cancers. *Internatinal Journal of Cancer* 128 (**2011**) 574-586.

6. Huang J.; Sengupta R.; Espejo A. B.; Lee M. G.; Dorsey J. A.; Richter M.; Opravil S.; Shiekhattar R.; Bedford M. T.; Jenuwein T.; Berger S. L. p53 is regulated by the lysine demethylase LSD1. *Nature* 449 (**2007**) 105-108.

7. Cho H. S.; Suzuki T.; Dohmae N.; Hayami S.; Unoki M.; Yoshimatsu M.; Toyokawa G.; Takawa M.; Chen T.; Kurash J. K.; Field H. I.; Ponder B. A.; Nakamura Y.; Hamamoto R. Demethylation of RB regulator MYPT1 by histone demethylase LSD1 promotes cell cycle progression in cancer cells. *Cancer Res* 71 (**2011**) 655-660.

8. Lv T.; Yuan D.; Miao X.; Lv Y.; Zhan P.; Shen X.; Song Y. Over-Expression of LSD1 Promotes Proliferation, Migration and Invasion in Non-Small Cell Lung Cancer. *PLoS ONE* 7 (**2012**) e35065.

9. Sorna V.; Theisen E. R.; Stephens B.; Warner S. L.; Bearss D. J.; Vankayalapati H.; Sharma S. High-Throughput Virtual Screening Identifies Novel N′-(1-Phenylethylidene)-benzohydrazides as Potent, Specific, and Reversible LSD1 Inhibitors. *Journal of Medicinal Chemistry* 56 (**2013**) 9496-9508.

10. Yu Y.; Wang B.; Zhang K.; Lei Z.; Guo Y.; Xiao H.; Wang J.; Fan L.; Lan C.; Wei

Y.; Ma Q.; Lin L.; Mao C.; Yang X.; Chen X.; Li Y.; Bai Y.; Chen D. High expression of lysine-specific demethylase 1 correlates with poor prognosis of patients with esophageal squamous cell carcinoma. *Biochemical and Biophysical Research Communications* 437 (**2013**) 192-198.

11. *Lynch J. T., et al.* LSD1 inhibition: a therapeutic strategy in cancer? *Expert Opinion on Therapeutic Targets* 16 (**2012**) 1239-1249.

12. Speranzini V.; Rotili D.; Ciossani G.; Pilotto S.; Marrocco B.; Forgione M.; Lucidi A.; Forneris F.; Mehdipour P.; Velankar S.; Mai A.; Mattevi A. Polymyxins and quinazolines are LSD1/KDM1A inhibitors with unusual structural features. *Science Advances* 2 (**2016**) e1601017.

13. Zheng Y.-C.; Shen D.-D.; Ren M.; Liu X.-Q.; Wang Z.-R.; Liu Y.; Zhang Q.-N.; Zhao L.-J.; Zhao L.-J.; Ma J.-L.; Yu B.; Liu H.-M. Baicalin, a natural LSD1 inhibitor. *Bioorganic Chemistry* 69 (**2016**) 129-131.

14. Duan Y.-C.; Guan Y.-Y.; Zhai X.-Y.; Ding L.-N.; Qin W.-P.; Shen D.-D.; Liu X.-Q.; Sun X.-D.; Zheng Y.-C.; Liu H.-M. Discovery of resveratrol derivatives as novel LSD1 inhibitors: Design, synthesis and their biological evaluation. *European Journal of Medicinal Chemistry* 126 (**2017**) 246-258.

15. Han C.; Li Z.; Hou J.; Wang Z.; Xu D.; Xue G.; Kong L. Bioactivity evaluation of natural product α-mangostin as a novel xanthone-based lysine-specific demethylase 1 inhibitor to against tumor metastasis. *Bioorganic Chemistry* 76 (**2018**) 415-419.

16. C. Zheng Y.; Yu B.; Z. Jiang G.; J. Feng X.; X. He P.; Y. Chu X.; Zhao W.; M. Liu H. Irreversible LSD1 Inhibitors: Application of Tranylcypromine and Its Derivatives in Cancer Treatment. *Current Topics in Medicinal Chemistry* 16 (**2016**) 2179-2188.

17. Zheng Y.-C.; Chang J.; Zhang T.; Suo F.-Z.; Chen X.-B.; Liu Y.; Zhao B.; Yu B.; Liu H.-M. An Overview on Screening Methods for Lysine Specific Demethylase 1 (LSD1) Inhibitors. *Current Medicinal Chemistry* 24 (**2017**) 2496-2504.

18. Kutz C. J.; Holshouser S. L.; Marrow E. A.; Woster P. M. 3,5-Diamino-1,2,4-triazoles as a novel scaffold for potent, reversible LSD1 (KDM1A) inhibitors. *MedChemComm* 5 (**2014**) 1863-1870.

19. Maes T.; Carceller E.; Salas J.; Ortega A.; Buesa C. Advances in the development

of histone lysine demethylase inhibitors. *Current Opinion in Pharmacology* 23 (**2015**) 52-60.

20. Maes T.; Mascaró C.; Ortega A.; Lunardi S.; Ciceri F.; Somervaille T. C. P.; Buesa C. KDM1 histone lysine demethylases as targets for treatments of oncological and neurodegenerative disease. *Epigenomics* 7 (**2015**) 609-626.

21. Sharma S. K.; Wu Y.; Steinbergs N.; Crowley M. L.; Hanson A. S.; Casero R. A.; Woster P. M. (Bis)urea and (Bis)thiourea Inhibitors of Lysine-Specific Demethylase 1 as Epigenetic Modulators. *Journal of Medicinal Chemistry* 53 (**2010**) 5197-5212.

22. Sharma S. K.; Hazeldine S.; Crowley M. L.; Hanson A.; Beattie R.; Varghese S.; Senanayake T. M. D.; Hirata A.; Hirata F.; Huang Y.; Wu Y.; Steinbergs N.; Murray-Stewart T.; Bytheway I.; Casero R. A.; Woster P. M. Polyamine-based small molecule epigenetic modulators. *MedChemComm* 3 (**2012**) 14-21.

23. Li Z.; Ding L.; Li Z.; Wang Z.; Suo F.; Shen D.; Zhao T.; Sun X.; Wang J.; Liu Y.; Ma L.; Zhao B.; Geng P.; Yu B.; Zheng Y.; Liu H. Development of the triazole-fused pyrimidine derivatives as highly potent and reversible inhibitors of histone lysine specific demethylase 1 (LSD1/KDM1A). *Acta Pharmaceutica Sinica B*, **2019**, DOI: 10.1016/j.apsb.2019.01.001.

24. Prusevich P.; Kalin J. H.; Ming S. A.; Basso M.; Givens J.; Li X.; Hu J.; Taylor M. S.; Cieniewicz A. M.; Hsiao P.-Y.; Huang R.; Roberson H.; Adejola N.; Avery L. B.; Casero R. A.; Taverna S. D.; Qian J.; Tackett A. J.; Ratan R. R.; McDonald O. G.; Feinberg A. P.; Cole P. A. A Selective Phenelzine Analogue Inhibitor of Histone Demethylase LSD1. *ACS Chemical Biology* 9 (**2014**) 1284-1293.

25. Lee H. T.; Choi M. R.; Doh M. S.; Jung K. H.; Chai Y. G. Effects of the monoamine oxidase inhibitors pargyline and tranylcypromine on cellular proliferation in human prostate cancer cells. *Oncology Reports* 30 (**2013**) 1587-1592.

26. Mimasu S.; Umezawa N.; Sato S.; Higuchi T.; Umehara T.; Yokoyama S. Structurally Designed trans-2-Phenylcyclopropylamine Derivatives Potently Inhibit Histone Demethylase LSD1/KDM1. *Biochemistry* 49 (**2010**) 6494-6503.

27. Zheng Y.-C.; Yu B.; Chen Z.-S.; Liu Y.; Liu H.-M. TCPs: privileged scaffolds for identifying potent LSD1 inhibitors for cancer therapy. *Epigenomics* 8 (**2016**) 651-666.

28. Mohammad Helai P.; Smitheman Kimberly N.; Kamat Chandrashekhar D.; Soong D.; Federowicz Kelly E.; Van Aller Glenn S.; Schneck Jess L.; Carson Jeffrey D.; Liu Y.; Butticello M.; Bonnette William G.; Gorman Shelby A.; Degenhardt Y.; Bai Y.; McCabe Michael T.; Pappalardi Melissa B.; Kasparec J.; Tian X.; McNulty Kenneth C.; Rouse M.; McDevitt P.; Ho T.; Crouthamel M.; Hart Timothy K.; Concha Nestor O.; McHugh Charles F.; Miller William H.; Dhanak D.; Tummino Peter J.; Carpenter Christopher L.; Johnson Neil W.; Hann Christine L.; Kruger Ryan G. A DNA Hypomethylation Signature Predicts Antitumor Activity of LSD1 Inhibitors in SCLC. *Cancer Cell* 28 (**2015**) 57-69.

29. Mohammad H.; Smitheman K.; Cusan M.; Liu Y.; Pappalardi M.; Federowicz K.; Van Aller G.; Kasparec J.; Tian X.; Suarez D.; Rouse M.; Schneck J.; Carson J.; McDevitt P.; Ho T.; McHugh C.; Miller W.; Johnson N.; Armstrong S. A.; Tummino P. Inhibition Of LSD1 As a Therapeutic Strategy For The Treatment Of Acute Myeloid Leukemia. *Blood* 122 (**2013**) 3964.

30. Milletti F.; Cheng W.-Y.; Maes T.; Lunardi S.; DeMario M.; Pierceall W. E.; Mack F. Abstract 4708: Neuroendocrine gene transcript expression is associated with efficacy to lysine-specific demethylase-1 inhibitor RG6016 in small cell lung cancer-derived cell lines. *Cancer Research* 76 (**2016**) 4708.

31. Lee S. H.; Stubbs M.; Liu X. M.; Diamond M.; Dostalik V.; Ye M.; Lo Y.; Favata M.; Yang G.; Gallagher K.; Leffet L.; He C.; Wu L.; Margulis A.; Covington M.; Wynn R.; Yao W.; Hollis G.; Huber R.; Ruggeri B.; Scherle P. Abstract 4712: Discovery of INCB059872, a novel FAD-directed LSD1 inhibitor that is effective in preclinical models of human and murine AML. *Cancer Research* 76 (**2016**) 4712.

32. Lee S. H.; Liu X. M.; Diamond M.; Dostalik V.; Favata M.; He C.; Wu L.; Wynn R.; Yao W.; Hollis G.; Huber R.; Scherle P.; Ruggeri B. Abstract 4704: The evaluation of INCB059872, an FAD-directed inhibitor of LSD1, in preclinical models of human small cell lung cancer. *Cancer Research* 76 (**2016**) 4704.

33. Zheng Y. C.; Shen D. D.; Ren M.; Liu X. Q.; Wang Z. R.; Liu Y.; Zhang Q. N.; Zhao L. J.; Zhao L. J.; Ma J. L.; Yu B.; Liu H. M. Baicalin, a natural LSD1 inhibitor. *Bioorg Chem* 69 (**2016**) 129-131.

34. Duan Y. C.; Guan Y. Y.; Zhai X. Y.; Ding L. N.; Qin W. P.; Shen D. D.; Liu X. Q.; Sun X. D.; Zheng Y. C.; Liu H. M. Discovery of resveratrol derivatives as novel LSD1 inhibitors: Design, synthesis and their biological evaluation. *Eur J Med Chem* 126 (**2017**) 246-258.

35. Ye X.-W.; Zheng Y.-C.; Duan Y.-C.; Wang M.-M.; Yu B.; Ren J.-L.; Ma J.-L.; Zhang E.; Liu H.-M. Synthesis and biological evaluation of coumarin–1,2,3-triazole–dithiocarbamate hybrids as potent LSD1 inhibitors. *MedChemComm* 5 (**2014**) 650-654.

36. Yu B.; Qi P.-P.; Shi X.-J.; Huang R.; Guo H.; Zheng Y.-C.; Yu D.-Q.; Liu H.-M. Efficient synthesis of new antiproliferative steroidal hybrids using the molecular hybridization approach. *European Journal of Medicinal Chemistry* 117 (**2016**) 241-255.

37. Wang B.; Zhao B.; Pang L.-P.; Zhao Y.-D.; Guo Q.; Wang J.-W.; Zheng Y.-C.; Zhang X.-H.; Liu Y.; Liu G.-Y.; Guo W.-G.; Wang C.; Li Z.-H.; Mao X.-J.; Yu B.; Ma L.-Y.; Liu H.-M. LPE-1, an orally active pyrimidine derivative, inhibits growth and mobility of human esophageal cancers by targeting LSD1. *Pharmacological Research* 122 (**2017**) 66-77.

38. Ma L.-Y.; Zheng Y.-C.; Wang S.-Q.; Wang B.; Wang Z.-R.; Pang L.-P.; Zhang M.; Wang J.-W.; Ding L.; Li J.; Wang C.; Hu B.; Liu Y.; Zhang X.-D.; Wang J.-J.; Wang Z.-J.; Zhao W.; Liu H.-M. Design, Synthesis, and Structure–Activity Relationship of Novel LSD1 Inhibitors Based on Pyrimidine–Thiourea Hybrids As Potent, Orally Active Antitumor Agents. *Journal of Medicinal Chemistry* 58 (**2015**) 1705-1716.

39. Zheng Y.-C.; Duan Y.-C.; Ma J.-L.; Xu R.-M.; Zi X.; Lv W.-L.; Wang M.-M.; Ye X.-W.; Zhu S.; Mobley D.; Zhu Y.-Y.; Wang J.-W.; Li J.-F.; Wang Z.-R.; Zhao W.; Liu H.-M. Triazole–Dithiocarbamate Based Selective Lysine Specific Demethylase 1 (LSD1) Inactivators Inhibit Gastric Cancer Cell Growth, Invasion, and Migration. *Journal of Medicinal Chemistry* 56 (**2013**) 8543-8560.

40. Li Z.-H.; Liu X.-Q.; Geng P.-F.; Suo F.-Z.; Ma J.-L.; Yu B.; Zhao T.-Q.; Zhou Z.-Q.; Huang C.-X.; Zheng Y.-C.; Liu H.-M. Discovery of [1,2,3]Triazolo[4,5-d]pyrimidine Derivatives as Novel LSD1 Inhibitors. *ACS*

Medicinal Chemistry Letters 8 (**2017**) 384-389.

41. Yu B.; Wang S.-Q.; Qi P.-P.; Yang D.-X.; Tang K.; Liu H.-M. Design and synthesis of isatin/triazole conjugates that induce apoptosis and inhibit migration of MGC-803 cells. *European Journal of Medicinal Chemistry* 124 (**2016**) 350-360.

42. Zheng Y. C.; Yu B.; Jiang G. Z.; Feng X. J.; He P. X.; Chu X. Y.; Zhao W.; Liu H. M. Irreversible LSD1 Inhibitors: Application of Tranylcypromine and Its Derivatives in Cancer Treatment. *Current Topics in Medicinal Chemistry* 16 (**2016**) 2179-2188.

43. Vianello P.; Botrugno O. A.; Cappa A.; Dal Zuffo R.; Dessanti P.; Mai A.; Marrocco B.; Mattevi A.; Meroni G.; Minucci S.; Stazi G.; Thaler F.; Trifiró P.; Valente S.; Villa M.; Varasi M.; Mercurio C. Discovery of a Novel Inhibitor of Histone Lysine-Specific Demethylase 1A (KDM1A/LSD1) as Orally Active Antitumor Agent. *Journal of Medicinal Chemistry* 59 (**2016**) 1501-1517.

44. Sartori L.; Mercurio C.; Amigoni F.; Cappa A.; Fagá G.; Fattori R.; Legnaghi E.; Ciossani G.; Mattevi A.; Meroni G.; Moretti L.; Cecatiello V.; Pasqualato S.; Romussi A.; Thaler F.; Trifiró P.; Villa M.; Vultaggio S.; Botrugno O. A.; Dessanti P.; Minucci S.; Zagarrí E.; Carettoni D.; Iuzzolino L.; Varasi M.; Vianello P. Thieno[3,2-b]pyrrole-5-carboxamides as New Reversible Inhibitors of Histone Lysine Demethylase KDM1A/LSD1. Part 1: High-Throughput Screening and Preliminary Exploration. *Journal of Medicinal Chemistry* 60 (**2017**) 1673-1692.

45. Vianello P.; Sartori L.; Amigoni F.; Cappa A.; Fagá G.; Fattori R.; Legnaghi E.; Ciossani G.; Mattevi A.; Meroni G.; Moretti L.; Cecatiello V.; Pasqualato S.; Romussi A.; Thaler F.; Trifiró P.; Villa M.; Botrugno O. A.; Dessanti P.; Minucci S.; Vultaggio S.; Zagarrí E.; Varasi M.; Mercurio C. Thieno[3,2-b]pyrrole-5-carboxamides as New Reversible Inhibitors of Histone Lysine Demethylase KDM1A/LSD1. Part 2: Structure-Based Drug Design and Structure–Activity Relationship. *Journal of Medicinal Chemistry* 60 (**2017**) 1693-1715.

46. Wu F.; Zhou C.; Yao Y.; Wei L.; Feng Z.; Deng L.; Song Y. 3-(Piperidin-4-ylmethoxy)pyridine Containing Compounds Are Potent Inhibitors of Lysine Specific Demethylase 1. *Journal of Medicinal Chemistry* 59 (**2016**) 253-263.

47. Mould D. P.; Alli C.; Bremberg U.; Cartic S.; Jordan A. M.; Geitmann M.;

Maiques-Diaz A.; McGonagle A. E.; Somervaille T. C. P.; Spencer G. J.; Turlais F.; Ogilvie D. Development of (4-Cyanophenyl)glycine Derivatives as Reversible Inhibitors of Lysine Specific Demethylase 1. *Journal of Medicinal Chemistry* 60 (**2017**) 7984-7999.

48. Nowotarski S. L.; Pachaiyappan B.; Holshouser S. L.; Kutz C. J.; Li Y.; Huang Y.; Sharma S. K.; Casero R. A.; Woster P. M. Corrigendum to "Structure–activity study for (bis)ureidopropyl- and (bis)thioureidopropyldiamine LSD1 inhibitors with 3-5-3 and 3-6-3 carbon backbone architectures" [Bioorg. Med. Chem. 23 (2015) 1601–1612]. *Bioorganic & Medicinal Chemistry* 26 (**2018**) 3728-3729.

49. Hayward D.; Cole P. A. LSD1 Histone Demethylase Assays and Inhibition. *Methods in enzymology* 573 (**2016**) 261-278.

50. Carradori S.; Petzer J. P. Novel monoamine oxidase inhibitors: a patent review (2012 - 2014). *Expert Opinion on Therapeutic Patents* 25 (**2015**) 91-110.

51. Wang S.; Zhao L.-J.; Zheng Y.-C.; Shen D.-D.; Miao E.-F.; Qiao X.-P.; Zhao L.-J.; Liu Y.; Huang R.; Yu B.; Liu H.-M. Design, synthesis and biological evaluation of [1,2,4]triazolo[1,5-a]pyrimidines as potent lysine specific demethylase 1 (LSD1/KDM1A) inhibitors. *European Journal of Medicinal Chemistry* 125 (**2017**) 940-951.

52. Burg J. M.; Gonzalez J. J.; Maksimchuk K. R.; McCafferty D. G. Lysine-Specific Demethylase 1A (KDM1A/LSD1): Product Recognition and Kinetic Analysis of Full-Length Histones. *Biochemistry* 55 (**2016**) 1652-1662.

53. Zhang X.; Zhang X.; Yu B.; Hu R.; Hao L. Oncogene LSD1 is epigenetically suppressed by miR-137 overexpression in human non-small cell lung cancer. *Biochimie* 137 (**2017**) 12-19.

54. Jafari R.; Almqvist H.; Axelsson H.; Ignatushchenko M.; Lundbäck T.; Nordlund P.; Molina D. M. The cellular thermal shift assay for evaluating drug target interactions in cells. *Nature Protocols* 9 (**2014**) 2100.

55. Wang M.; Liu X.; Guo J.; Weng X.; Jiang G.; Wang Z.; He L. Inhibition of LSD1 by Pargyline inhibited process of EMT and delayed progression of prostate cancer in vivo. *Biochemical and Biophysical Research Communications* 467 (**2015**) 310-315.

56. Lin T.; Ponn A.; Hu X.; Law B. K.; Lu J. Requirement of the histone demethylase LSD1 in Snai1-mediated transcriptional repression during epithelial-mesenchymal transition. *Oncogene* 29 (**2010**) 4896-4904.

57. Forneris F.; Binda C.; Adamo A.; Battaglioli E.; Mattevi A. Structural Basis of LSD1-CoREST Selectivity in Histone H3 Recognition. *Journal of Biological Chemistry* 282 (**2007**) 20070-20074.

58. Yu B.; Shi X.-J.; Zheng Y.-F.; Fang Y.; Zhang E.; Yu D.-Q.; Liu H.-M. A novel [1,2,4] triazolo [1,5-a] pyrimidine-based phenyl-linked steroid dimer: Synthesis and its cytotoxic activity. *European Journal of Medicinal Chemistry* 69 (**2013**) 323-330.

Highlights

- A new series of [1,2,4]triazolo[1,5-*a*]pyrimidine derivatives were designed and synthesized as new LSD1 inhibitors.
- **C26** inhibited LSD1 reversibly and showed selectivity to LSD1 over MAO-A/B.
- In LSD1 overexpressed A549 cells, compound
- **C26** concentration-dependently induced accumulation of H3K4me1/me2 and H3K9me2 and showed cellular target engagement to LSD1 in A549 cells.
- **C26** significantly inhibited migration of A549 cells in a concentration-dependent manner.
- The [1,2,4]triazolo[1,5-*a*]pyrimidine could serve as a promising scaffold for the development of new LSD1 inhibitors.